ELSEVIER

PALAEO

Palaeogeography, Palaeoclimatology, Palaeoecology 178 (2002) 321–345

www.elsevier.com/locate/palaeo

Trace elements, stable isotopes, and clay mineralogy of the Elles II K–T boundary section in Tunisia: indications for sea level fluctuations and primary productivity

D. Stüben [a,*], U. Kramar [a], Z. Berner [a], W. Stinnesbeck [b], G. Keller [c], T. Adatte [d]

[a] *Institut für Petrographie und Geochemie, Universität Karlsruhe, Postfach 6980, D-76128 Karlsruhe, Germany*
[b] *Geologisches Institut, Universität Karlsruhe, Postfach 6980, D-76128 Karlsruhe, Germany*
[c] *Department of Geosciences, Princeton University, Princeton, NJ 08544, USA*
[d] *Institut de Géologie, 11 Rue Emile Argand, 2007 Neuchâtel, Switzerland*

Received 12 October 1999; accepted 17 August 2001

Abstract

Trace elements and stable isotopes in bulk rocks and foraminifera, bulk rock and clay mineral compositions, are used as palaeoproxies to evaluate sea level fluctuations, climatic changes and variations in primary productivity across the K–T transition at Elles II in Tunisia from 1 m (~33 kyr) below to 1 m (~70 kyr) above the K–T boundary. Results on clay minerals, major and trace elements, stable isotopes in bulk rock samples (e.g. Ca, Cu, Zn, Rb, Sr, Zr, Ba, $\delta^{13}C$ and $\delta^{18}O$), and in foraminifera (Sr/Ca, $\delta^{13}C$, $\delta^{18}O$) indicate that the latest Maastrichtian (last ~33 kyr) in Tunisia was marked by a relatively warm, but humid climate and a rising sea level. The transgressive surface is marked by deposition of a foraminiferal packstone just below the K–T boundary followed by maximum flooding across the K–T boundary (red layer and black clay layer). Humid warm conditions accompanied the maximum flooding, along with increased total organic carbon values and rapidly decreasing primary productivity. At the K–T boundary, an impact event (Ir anomaly, Ni-rich spinels, spherules) exacerbated already stressed environmental conditions leading to the mass extinction of tropical planktic foraminifera. Increasingly more humid conditions prevailed within the lowermost Danian Zone P0 (~50 kyr) culminating in a sea level lowstand near the top of P0. A slow recovery of the ecosystem in Zone P1a coincided with a rising sea level and gradually less humid climatic conditions.

Keywords: palaeoceanography; geochemistry; stable isotopes; trace elements; foraminifera

1. Introduction

The Cretaceous–Tertiary (K–T) profile at Elles II is one of the rare complete K–T transitions in Tunisia, similar to the El Kef stratotype. Across the K–T boundary dramatic changes in planktic foraminiferal faunas, including the mass extinction of tropical species, as well as major changes in lithology, sea level and climatically induced variations in primary productivity coincide with evidence of a

* Corresponding author. Fax: +49-721-608-7247.
E-mail address: doris.stueben@bio-geo.uni-karlsruhe.de (D. Stüben).

0031-0182/02/$ – see front matter
PII: S0031-0182(01)00401-1

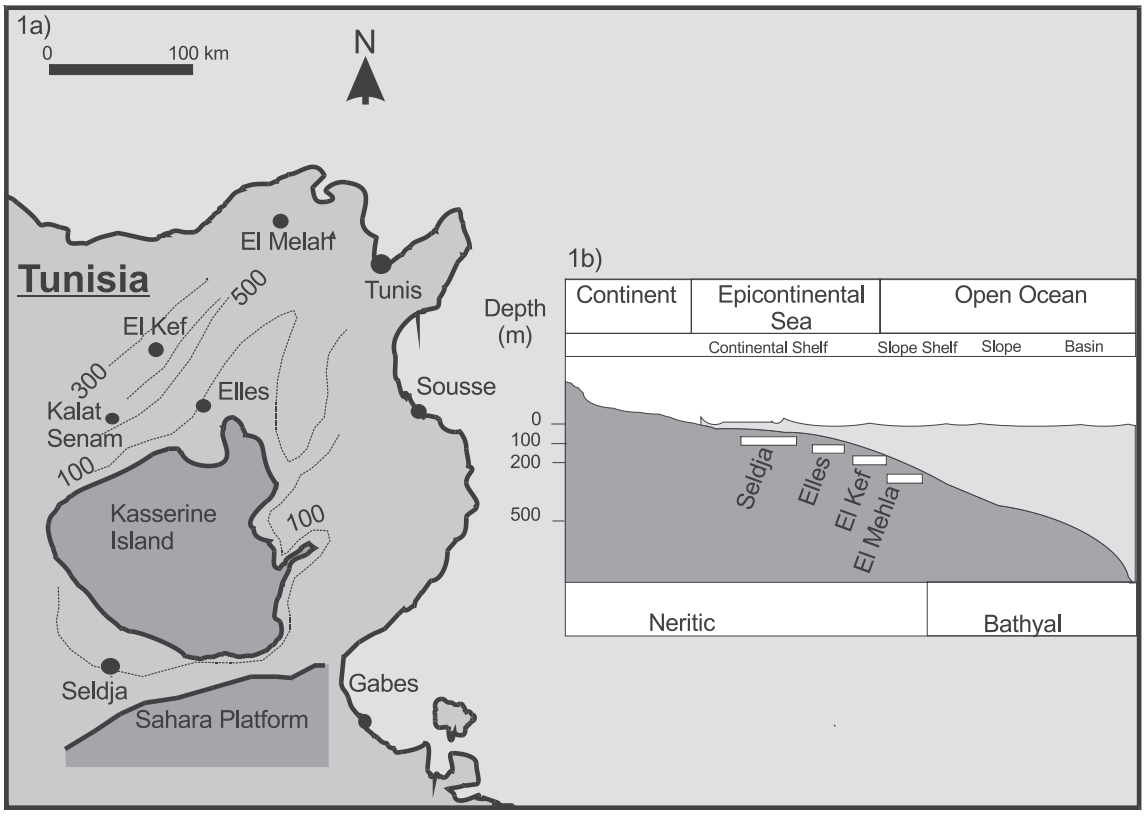

Fig. 1. (a) Location map of the Elles section in northwestern Tunisia (modified after Burollet, 1967). (b) Schematic cross-section with positions of the Seldja, Elles, El Kef and El Melah K–T sections.

catastrophic impact event (e.g. Ir anomaly, spherules, Ni-rich spinels) (e.g. Smit, 1982; Keller et al., 1996, 2002; Rocchia et al., 1995). Biotic and environmental consequences associated with the K–T transition are well known from deeper water (shelf, slope) marine environments where sediment accumulation rates were relatively high and exposure to erosion was limited to submarine current activity. In northern Tunisia, a number of such deeper water sections are known including El Kef, Ain Settara (Kalaat Senan) and El Melah (Fig. 1). To the south, sediment deposition occurred in shallow areas adjacent to the Sahara platform (Keller et al., 1998).

The El Kef section, which is designated the K–T boundary stratotype section, has been studied by numerous authors (e.g. Perch-Nielsen, 1981; Donze et al., 1982, 1985; Smit, 1982; Peypouquet et al., 1986; Keller, 1998; Brinkhuis and Zachariasse, 1988; Méon, 1990; Saint-Marc, 1992; Pospichal, 1994; Ben Abdelkader and Zargouni, 1995; Rocchia et al., 1995; Keller et al., 1996; Kouwenhoven et al., 1997).

The El Kef stratotype outcrop is currently rather depleted by oversampling and eroded by agricultural encroachment. For these reasons, a group of scientists assembled during the International Workshop on Cretaceous–Tertiary Transitions in Tunis, 1998, and sampled the Elles and Ain Settara sections as possible additional or alternative stratotypes (Remane et al., 1999). Since that time, various studies have found that the Elles section is one of the rare complete K–T transitions in Tunisia, similar to the El Kef stratotype, but possibly more expanded (Karoui and Zaghbib-Turki, 1998; Karoui-Yakoub et al., 2002).

The Elles section is located between El Kef to the northwest and the Kasserine Island to the south (Fig. 1a). Sediment deposition occurred at middle to outer neritic depths, slightly deeper

than the nearby Ain Settara section (Molina et al., 1998; Luciani, 2002), and significantly deeper than the Seldja section to the south located in a channel between the Kasserine Island and the Sahara platform (Fig. 1b). We report here the results of detailed geochemical and isotopic studies of the Elles II K–T transition which provide an important database for reconstructing palaeoclimatic and palaeoenvironmental conditions.

1.1. Trace elements as palaeoproxies

Palaeoproxies, such as C and O isotopes as well as nutrient-type trace elements, have been used to reconstruct changes in oceanic circulation patterns, climate and primary productivity (e.g. Shackelton et al., 1983; Broecker and Peng, 1984; Boyle, 1986; Fischer and Wefer, 1999). Bio productivity is mainly controlled by the availability of nutrients. Trace elements, such as P, Ba and S, and some heavy metals (e.g. Cu, Ni, Zn, Cd) are known to be involved in the biogenic cycle as micro- or nanonutrients and consequently they tend to correlate with the bioproductivity (Knauer and Martin, 1982), whereas Ti, Zr and Al are correlated with detrital influx. Concentrations of nutrient-associated elements in the water column are controlled by the rate of primary productivity in surface waters. In the water column Cd, P and $\delta^{13}C$ are linearly correlated (Boyle, 1986). In biogenic sediments, variations of Ba (Dymond et al., 1992; Schroeder et al., 1997), P and some heavy metals (e.g. von Breymann et al., 1992; Brasier, 1995), Cd/Ca ratios and $\delta^{13}C$ in foraminiferal shells (e.g. Boyle, 1986; Rosenthal et al., 1997a) have been variously used as proxies for primary palaeoproductivity. For example, total Ba content in sediments depends on primary productivity, the amount of the terrigenous detrital component (Murray and Leinen, 1996; Schroeder et al., 1997), and on post-depositional barite preservation (McManus et al., 1998, 1999; Gingele et al., 1999). The influence of terrigenous components on the concentrations of some trace elements used as palaeoproxy can be corrected by means of El/Al or El/Ti ratios, where El is the respective element (e.g. Murray and Leinen, 1996; Schroeder et al., 1997; Gingele et al., 1999). In oligotrophic areas and well above the lysocline, carbonate accumulation can also serve as an indicator of palaeoproductivity (Rühlemann et al., 1996; Dittert et al., 1999).

Strontium is a useful proxy for sea level changes. At times of falling sea levels, Sr-rich aragonite from continental shelves is exposed to weathering and alters to calcite. During these times, most of the Sr is relatively rapidly released to the oceans (within about 100 000 years). Sea level fluctuations are therefore related to variations in the Sr content of the sediments (e.g. Graham et al., 1982; Stoll and Schrag, 1996, 1998; Li et al., 2000). Rathburn and Dedeckker (1997) report a correlation of Mg/Ca and Sr/Ca ratios with temperature in shells from the recent benthic foraminifer *Cibicidoides*. In contrast, Rosenthal et al. (1997b) observed no correlation with temperature, but a strictly linear decrease with water depth, which they explained as pressure dependence. Because pressure is proportional to water depth, the pressure effect amplifies the signal from sea level-derived Sr concentrations in seawater for benthic foraminifera. Thus, the Sr/Ca ratio in calcite shells of foraminifera, which depends on the Sr concentration of the palaeo-seawater, is mainly controlled by sea level variations, salinity, ambient temperature and pressure.

Ratios of stable isotopes of O and C in calcareous tests of planktic foraminifera are widely used in palaeoceanography to reconstruct environmental parameters of ancient ocean surface waters, assuming that the isotopic signals of the shells reflect the isotopic characteristics of the ambient surface waters in which they formed. The O isotope composition of planktic foraminifera is believed to accurately record $\delta^{18}O$ variations of the ambient seawater and hence variations of temperature, based on the assumption that planktic foraminifera build their tests in isotopic equilibrium with ambient seawater (Epstein et al., 1953; Shackelton, 1967; Erez and Luz, 1992). The $\delta^{13}C$ ratios of planktic and benthic calcareous tests reflect the isotopic composition of dissolved CO_2 in ambient seawater, if formed under equilibrium conditions. Photosynthesis in the photic zone, dissolution of calcareous tests, organic carbon mineralisation, and CO_2 regeneration in deep waters

cause a vertical carbon isotope gradient in a way that generally heavier $\delta^{13}C$ values are found in planktic and lighter values in benthic tests. The shift within the $\delta^{13}C$ history of planktic and benthic foraminifera indicate either the occurrence of different carbon reservoirs in the global carbon cycle, or a change in the intensity of the ocean surface productivity (e.g. Shackelton, 1987).

2. Geological setting and lithology

The Elles II section is located in the Karma valley near the hamlet of Elles, about 75 km SE of the town of El Kef (Fig. 1). Upper Maastrichtian sediments are dominated by grey marls, siltstones, and shales which were deposited in middle to outer neritic environments with a water depth of approximately 100–200 m at Elles. Occasional Fe-rich concretions ranging up to 1 cm in diameter and composed mainly of goethite and jarosite are present. These minerals are of secondary origin and reflect late diagenetic processes. Many intervals are mottled because of ichnofaunal activity, but individual traces are rarely preserved because of the soft pelitic sediment. In several horizons, however, *Chondrites, Planolites* and possibly *Teichichnus* were identified; megafossils appear to be absent. A sedimentological change to a bioclastic deposit occurs at the top of the Maastrichtian succession. Between 30 and 15 cm below the K–T boundary grey marls grade into grey calcareous siltstones and then into a 5–8 cm thick grey calcarenite. Above this interval and up to 1–2 cm below the K–T boundary is a 5–7 cm thick yellow calcarenite which consists primarily of planktic foraminiferal tests (foraminiferal packstone). This sediment is cross-bedded, burrowed and an undulating upper surface marks an erosional disconformity. Burrows are approximately 5 mm in diameter, unbranched, and reach a length of a few centimetres. Most burrows are horizontal or oblique, but a few almost vertical shafts initiate in the upper surface of the bioclastic layer. All burrows, even the vertical shafts, are packed with yellow foraminiferal sand, rather than the green clay that overlies the calcarenitic layer and erosional contact. No exotic minerals are observed within this bioclastic deposit and its physical characteristics reveal no similarities with tsunami deposits (Stinnesbeck et al., 1998).

Biostratigraphically this bioclastic deposit is near the top of planktic foraminiferal zone CF1 (*Plummerita hantkeninoides*), which spans the last 300 kyr of the Maastrichtian (Pardo et al., 1996; Keller et al., 2002). A plastic green clay, 0.2–1 cm thick, fills the depressions of the undulating upper surface of the calcarenite and underlies a 2–3 mm thin ferruginous red layer which marks the K–T boundary and contains an Ir anomaly, Ni-rich spinels, and spherules (Rocchia et al., 2002). The first Tertiary planktic foraminifera appear within the first 2–5 cm of clay above the red layer (Keller et al., 2002). No burrows appear to be present in the green clay and none cross the red layer. Overlying the red layer is a 2 cm thick plastic green clay that also contains a millimetre thick red layer. The green clay is overlain by a 10 cm thick black organic-rich clay that contains rare casts of nuculanid bivalves. Upsection, the black clay grades into dark fissile black shales with small Fe-rich concretions followed by grey and light grey shales which are less fissile for several metres upsection. Bioturbation first reappears at 50 cm above the K–T red layer.

2.1. Sediment accumulation rates

Of major concern for any K–T studies are the age and completeness of the section analysed. Numeric age control is generally based on magnetostratigraphy, though such data are not available for any of the Tunisian K–T boundary transitions. In the absence of such data, numeric ages for the Maastrichtian interval of the Elles II section were extrapolated by Li and Keller (1998a) based on biostratigraphic correlation with DSDP Site 525A, which has an excellent palaeomagnetic record. However, since the latest Maastrichtian Zone CF1 is not identified at Site 525A, because the zonal index species is restricted to lower latitudes, the duration of this zone was estimated based on the magnetostratigraphy of the Agost section as spanning the last 300 kyr of the Maastrichtian (chron 29R) (Pardo et al., 1996). Based on this age estimate, sedimentation rates averaged

2 cm/1000 yr at El Kef and 3 cm/1000 yr at Elles II for Zone CF1. The higher sedimentation rate at Elles II is due to its proximity to the Kasserine Island and the greater influx of terrigenous sediments.

Above the K–T boundary, the top of Zone P1a is correlated to the top of chron 29R. Estimating sediment accumulation rates for the P0 and P1a intervals, however, depends largely on which estimate for the duration of chron 29R above the K–T boundary is used: 230 kyr (Berggren et al., 1995), 268 kyr (Cande and Kent, 1992), 255 kyr (Cande and Kent, 1995), or 296 kyr (Herbert et al., 1995). In this study we adopt Cande and Kent (1995). At Elles II, Zones P0 and P1a span 6 m, whereas at El Kef the comparable interval spans 5 m. Based on Cande and Kent's (1995) age estimate, the time-averaged sediment accumulation rate for Elles II is 2.3 cm/1000 yr, as compared with 1.9 cm/1000 yr for El Kef. Estimating sediment accumulation rates separately for P0 and P1a, using a duration of 50 kyr for P0, yields an average sediment accumulation rate of 1 cm/1000 yr for P0 and 2.25 cm/1000 yr for P1a at Elles II. Across the thin K–T boundary red layer and thin black clay, strongly reduced sediment accumulation rates suggest a rate of deposition of probably no more than 0.1 cm/1000 yr. Based on these sedimentation accumulation rates, the Elles II interval (from −100 cm to +100 cm) encompassed the last ~33 kyr of the Cretaceous and the first ~70 kyr of the Tertiary.

3. Materials and methods

A total of 45 bulk samples were analysed from 1 m below to 1 m above the K–T boundary. Samples were taken at centimetre intervals across the K–T transition (clay and bioclastic layers) and at 10-cm intervals in the shales and marls above and below the boundary. Geochemical studies were conducted on the benthic foraminiferal species *Anomalinoides acuta* and planktic species *Rugoglobigerina rugosa*.

3.1. Bulk samples

In bulk samples, some major (Ca, Fe) and trace element contents (Cu, Zn, Rb, Sr, Zr, Ba and Pb) were analysed by energy-dispersive X-ray fluorescence (ED-XRF) with a Spectrace 5000, equipped with a Rh tube and Si (Li) detector (30 mm^2) following the analytical procedure described by Kramar (1984, 1997). To check measurement accuracy, the certified standards MRG-1, AGV-1, GXR-2, SGR-1, SOIL-5 and SOIL-7 were analysed within a batch. For all elements analysed in the bulk samples, our results were within 10% of the recommended values for the reference samples (Govindaraju, 1994). Detection limits for the trace elements and median values for bulk concentrations of the profile are given in Table 1.

Stable carbon and oxygen isotope data for carbonate were obtained from finely ground bulk samples using a fully automated preparation system (MultiCarb) connected on-line to an Optima isotope ratio mass spectrometer (Micromass Limited, UK). All carbon and oxygen isotope data are reported as δ values relative to the PDB standard, with reproducibility better than 0.1‰ (2s).

Mineralogical analyses of bulk rock samples were conducted at the Geological Institute of the University of Neuchatel, Switzerland, according to the methods described by Adatte et al. (1996) and Li et al. (2000).

3.2. Foraminiferal tests

Isotopic ratios of C and O in foraminiferal tests were determined separately on benthic (*Anomalinoides acuta*, 32 samples) and on planktic species (*Rugoglobigerina rugosa*, 15 samples). Foraminifera from the Elles II K–T profile are well pre-

Table 1
Limits of detection of ED-XRF for trace elements in bulk rock samples together with their median values within the profile

Element	Cu	Zn	Rb	Sr	Zr	Ba	Pb
Detection limit	5	4	0.8	0.7	2	3	2.5
Median	17	107	40	811	94	89	11

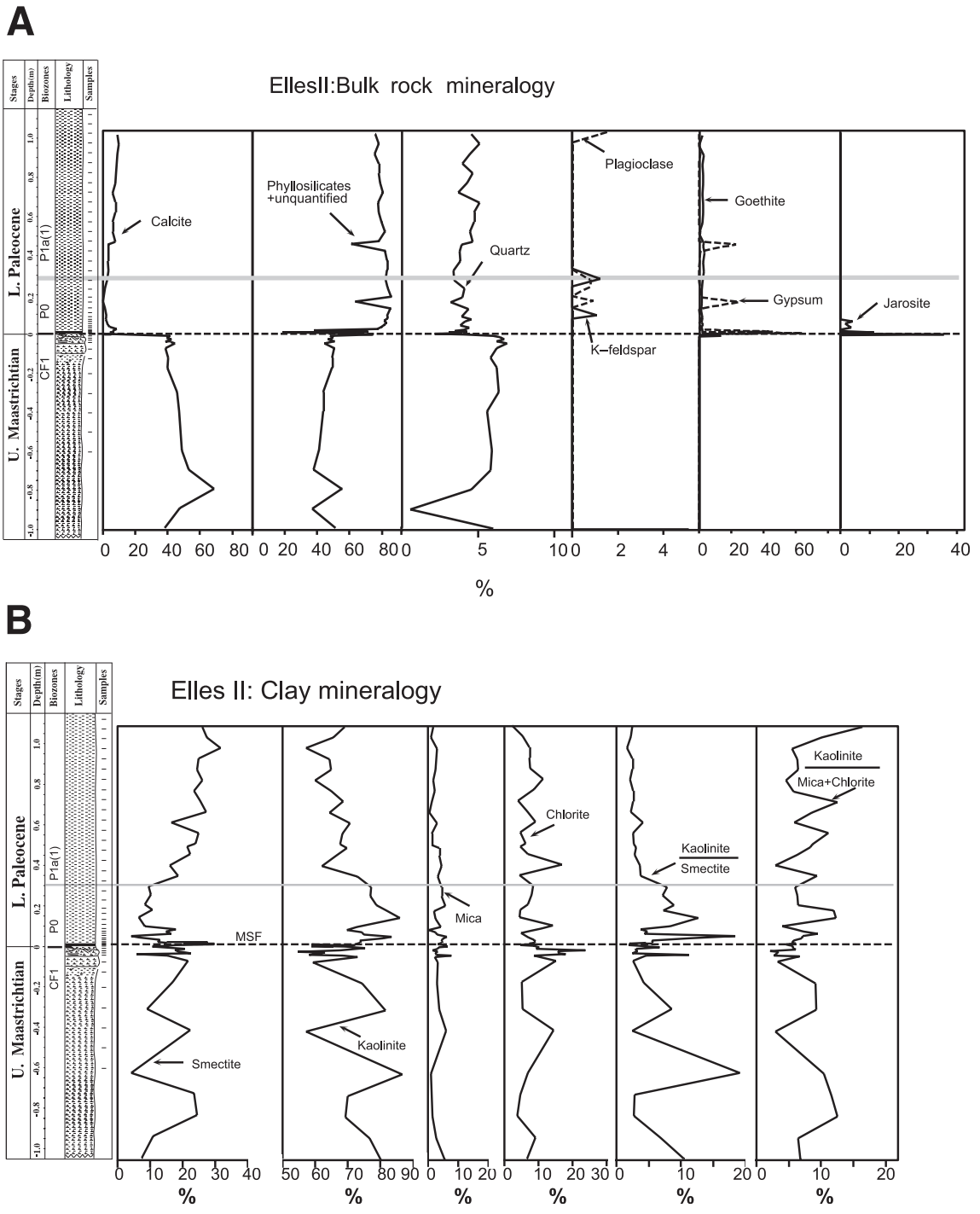

Fig. 2. (A) Bulk rock mineral composition across the K–T transition at Elles II. (B) Clay minerals across the K–T transition at Elles II and inferred sea level fluctuations and environmental conditions (e.g. humidity) across the K–T interval. FP = foraminiferal packstone, T = transgression, MSF = maximum flooding surface

served and show no signs of carbonate dissolution. Trace element contents were determined by means of total reflection X-ray fluorescence (T-XRF, Atomika EXTRA II) on 29 samples of benthic and nine samples of planktic foraminifera. One to six specimens, weighing 7.5–45 μg, which showed no visible inclusions of sediments or Fe-oxide coatings, were used for these analyses, but due to the lack of material no special cleaning procedure could be applied to the foraminiferal tests. They were cleaned with bidistilled water and transferred into PP microcentrifuge tubes. 100 μl subboiled HNO_3, spiked with 0.2 ng Ga/μl, was added to each sample as internal standard. The tubes than were centrifuged at approximately 10 000 RCF to concentrate sample and nitric acid in the cone of the microcentrifuge tubes. The samples were digested for 1 h in an ultrasonic bath and centrifuged again. 50 μl of each solution was transferred to the quartz sample carrier, dried and analysed for 2000 s by T-XRF using a Mo tube at 50 kV/38 mA and a Mo filter, and a W tube. The trace element contents were then normalised to Ca. The actual sample weights were calculated from the Ca content by means of the internal standard (Ga spike). Absolute detection limits of 10 pg to several hundred pg have been achieved for Mn, Ni, Cu and Zn. In almost all of the analysed samples, the Cd and Ba contents were below the detection limit, and for Cu, Mo, As, Rb, Y, and Zr very close to it. Heavy metal concentrations, especially Zn and Cu, but also elements bound to clay minerals like Rb and Y may be an artifact of incorporated sediment or invisible Fe–Mn coatings. Expected concentrations in foraminifera shells for these elements are approximately a factor 10 lower than in the bulk sediment, whereas Sr contents of foraminifera are at least a factor 10 higher than in bulk sediments. Therefore only Sr contents are considered reliable and were used in further interpretation.

4. Results

4.1. Whole-rock mineralogy

The uppermost 1 metre of the Maastrichtian, which corresponds to the uppermost part of Zone CF1 (Keller et al., 2002), is characterised by relatively high calcite and phyllosilicate contents which generally fluctuate between 40 and 60%, and minor quartz (4–6%). Feldspars, goethite, jarosite, and gypsum are not present in this part of the section (Fig. 2A). Maximum calcite (55–60%) is observed at 80 cm below the K–T boundary and values slightly decrease upward (40–45%). The yellow foraminiferal packstone, which ends at 1–2 cm below the K–T boundary, is marked by increased calcite (from 39 to 43%) and decreased detrital input. The overlying 0.2–1 cm thick plastic green clay, which fills the depressions of the foraminiferal packstone and immediately underlies the K–T boundary red layer, is marked by an abrupt drop in calcite (from 43% to 15%) and increased phyllosilicates. Above this interval, the K–T boundary clay layer is almost devoid of calcite (1–2%), but dominated by phyllosilicates (20–60%). Hydroxide minerals, such as jarosite (18%) and goethite (14%), are also present along with minor gypsum (4%). All these minerals are of secondary origin and reflect late diagenetic processes. Moreover, gypsum dominates with 65% in the upper part of the clay layer and in the overlying 0.5 cm. Upsection, the next 46 cm of clayey shale, which corresponds to Zone P0 and the base of P1a (1), are still characterised by very low calcite (less than 10%). Minor detrital components, such as quartz ($<4\%$), K-feldspars and plagioclase ($<2\%$), are also present along with minor amounts of goethite ($<5\%$) and sporadic gypsum. Upsection in Zone P1a (1), no significant bulk rock compositional changes are apparent, though calcite gradually increases to 10% (Fig. 2A).

Relative changes in bulk rock mineralogy reflect variations in sediment source, intensity of weathering and erosion under arid and humid climates, and the variable influx of terrigenous sediments into the oceans during high and low sea levels. Elles was located on the continental shelf-slope environment, close to the emerged areas of the Kasserine island (Burollet, 1956), as indicated by the generally higher influx of detrital components, such as phyllosilicates and quartz. The variations in the observed detrital influx primarily

indicate variable rates of weathering and erosion of terrestrial sediments associated with climate and sea level fluctuations. At Elles II, the K–T transition is marked by a sharp change in bulk rock composition (Fig. 2A) characterised by a drop in calcite and increased phyllosilicate contents. Secondary minerals such as gypsum, jarosite and goethite of late diagenetic origin are present near and within the K–T boundary layer. This abrupt decrease in calcite content could represent a drop in productivity of planktic carbonate, possibly caused by short- and long-term effects of a probable catastrophic event. Long-term effects are also seen in the increased phyllosilicate content which began well below the K–T boundary (see Adatte et al., 2002) and the increasing detrital input; both could be linked to long-term climatic changes towards more humid conditions which culminated 100–150 kyr after the K–T boundary.

4.2. Clay minerals

At Elles II, the clay mineral assemblages are dominated by kaolinite (50–90%), variable smectite (6–30%) and chlorite (2–25%), and minor mica (0–5%) (Fig. 2B). Kaolinite is very abundant in the uppermost Maastrichtian with a maximum (90%) at 60 cm below the K–T boundary and similarly peak values are observed in Zone P0. Repeated kaolinite/smectite fluctuations, from 60 to 90% and 10 to 25%, are observed at 100 cm and 50 cm below the K–T boundary, respectively. The calcarenite (foraminiferal packstone, 1–7 cm below K–T) is marked by high kaolinite (69–75%), variable smectite (10–20%), and a maximum in chlorite (24%). The plastic green clay and K–T boundary black clay are marked by a significant increase in smectite (up to 30%), decreased kaolinite (down to 60%) and chlorite. The smectite from the K–T layer is identical to the smectite within uppermost Maastrichtian and lowermost Danian sediments. Its Fe–Al composition is not very well crystallised and it typically develops in soils under intermediate climatic conditions with seasonal contrasts (Chamley, 1989). Upsection, clayey shales of Zone P0 show a significant decrease in smectite which coincides with maximum kaolinite contents. Smectite gradually increases upsection in Zone P1a (1), coincident with decreasing kaolinite.

Clay mineral assemblages can reflect continental morphology and tectonic activity as well as climate evolution and associated sea level fluctuations (Chamley, 1989; Weaver, 1989; Li et al., 2000). Mica and chlorite are considered common by-products of weathering reactions with low hydrolysis, typical of cool to temperate and/or dry climates. Kaolinite is generally a by-product of highly hydrolytic weathering reactions in perennially warm humid climates and its formation requires a minimum of 15°C (Gaucher, 1981). Smectite in oceanic sediments can originate from volcanogenic, diagenetic and detrital sources. The sediments in the Elles section did not suffer deep burial diagenesis. The absence of a significant diagenetic overprint is documented by the constant but variable presence of smectite, the near absence of mixed-layer illite–smectite, and the co-existence of smectite with a high kaolinite content in different parts of the section (Fig. 2B). Authigenic smectite can form locally in deep sea environments during hydrothermal weathering of volcanic rocks (Karpoff et al., 1989; Chamley, 1989). But these kinds of rocks are not abundant in this part of the African margin. Smectite is therefore interpreted as mainly of detrital origin and may be used as marker of a warm climate, with alternating wet and dry seasons (Chamley, 1989). On the other hand, it has been shown

Fig. 3. (A) Variations of CaO, Sr, Rb, Zn, Zr and Ba of bulk samples from 1 m above and 1 m below the K–T boundary of the Elles II section. (B) Elemental flux of CaO, Sr, Rb, Cu, Zn, Zr and Ba estimated from bulk samples from 1 m above and 1 m below the K–T boundary of the Elles II section. Assumed sedimentation rates: 3 cm/1000 yr for the Maastrichtian; 0.1 cm/1000 yr for the Red Layer and the thin black clays below; 1 cm/1000 yr during Zone P0, and 2.25 cm/1000 yr during Zone P1a (1). The sediment density was assumed to be 2.4 g/cm^3 for clayey and siliciclastic sediments corrected for the carbonates and Fe-oxides, assuming a density of 3.0 g/cm^3 for carbonates and 4.5 g/cm^3 for Fe-oxides.

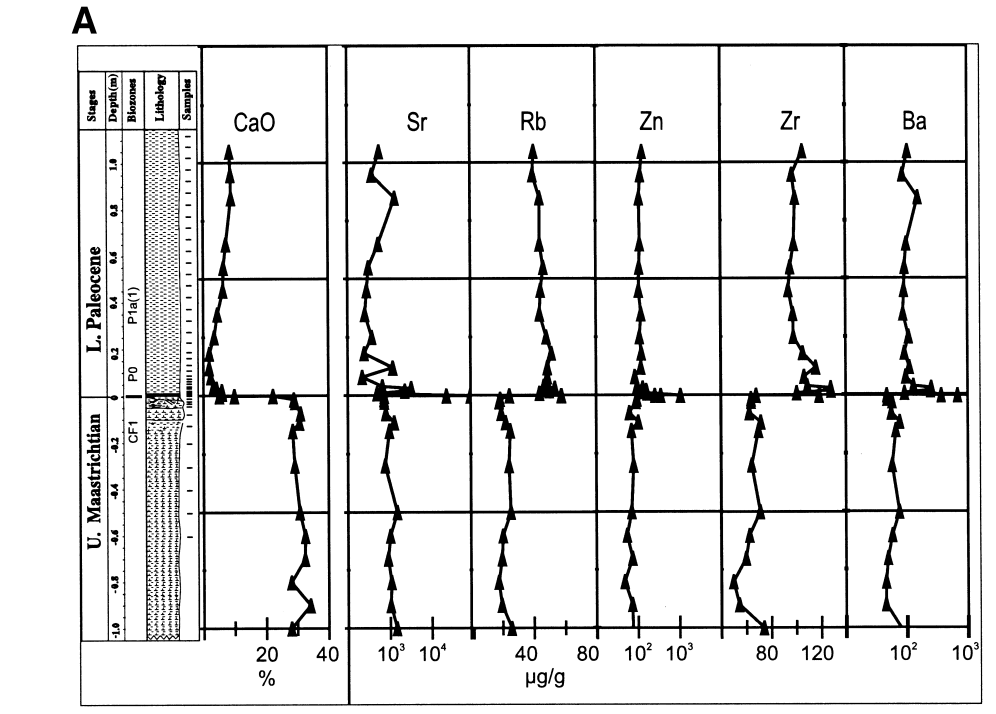
A
Stages
Depth(m)
Biozones
Lithology
Samples
L. Paleocene
U. Maastrichtian
P1a(1)
P0
CF1
CaO
Sr
Rb
Zn
Zr
Ba
20 40
%
10³ 10⁴
40 80
10² 10³
80 120
10² 10³
µg/g

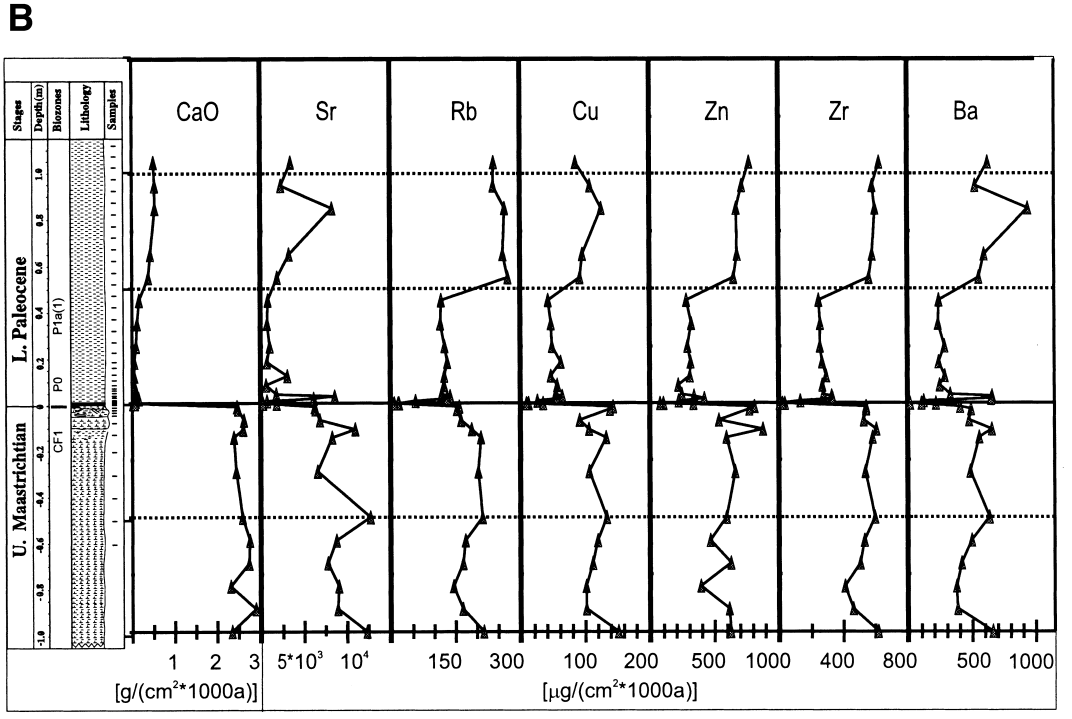
B
Stages
Depth(m)
Biozones
Lithology
Samples
L. Paleocene
U. Maastrichtian
P1a(1)
P0
CF1
CaO
Sr
Rb
Cu
Zn
Zr
Ba
1 2 3
5*10³ 10⁴
150 300
100 200
500 1000
400 800
500 1000
[g/(cm²*1000a)]
[µg/(cm²*1000a)]

that maximum amounts of smectite frequently coincide with long-term or short-term high sea levels (Debrabant et al., 1992; Deconinck, 1992), and hence can also be used as a proxy for sea level fluctuations.

The distribution of kaolinite and smectite in marine sediments of Tunisia may be partly related to the distance from the shoreline, as well as to sea level changes. Clay mineral segregation by differential settling processes is commonly observed in Cretaceous sediments where large carbonate platforms grade over short distances into deep basins (Chamley and Masse, 1975; Deconinck et al., 1985; Adatte and Rumley, 1989). The main mechanism responsible for this segregation appears to be grain size sorting, with smectite consisting generally of smaller particles than kaolinite (Gibbs, 1977; Chamley, 1989; Hendriks et al., 1990).

During the latest Maastrichtian to early Danian, the Tunisian sections were located on a continental platform with direct access to the open sea, and thus, they experienced no significant hydrodynamic activity and hence little mineral segregation that could mask or exaggerate the climate signal (Monaco et al., 1982; Adatte and Rumley, 1989; Chamley, 1989). Since kaolinite is more abundant in coastal areas and smectite in open marine environments, kaolinite/smectite (K/SM) ratios may also reflect sea level changes (Chamley et al., 1990). But primarily, variations in K/SM are linked to climate changes. The K/SM ratio is therefore a climate proxy that reflects humid and warm to more dry and seasonal climate variations (e.g. Robert and Chamley, 1991; Robert and Kennett, 1994), whereas the kaolinite/(chlorite+mica) index represents an estimate of cold to temperate-dry and warm-humid climates.

At Elles, the uppermost metre of the Maastrichtian, corresponding to the upper part of Zone CF1, is marked by high but variable kaolinite, suggesting very humid conditions and accelerated terrigenous runoff during a sea level lowstand. The general increase in clay minerals of different origins, which coincided with the deposition of the foraminiferal packstone just below the K–T boundary, suggests a rise in sea level (Fig. 2B), though the kaolinite–smectite fluctuations in this interval (1–5 cm below the K–T boundary) may reflect sea level and climate variations of short duration. The increased smectite in the plastic green clay and overlying K–T boundary clay layer suggests a condensed interval due to a rising sea level (maximum flooding) and more seasonal climate (Chamley et al., 1990), rather than weathering of fallout impact products, such as glass. The spikes in the K/SM ratio within Zone P0 may reflect increasing humidity and a possible warming amid a higher sea level. Similar spikes have also been reported in several other coeval Tunisian sections (Adatte et al., 2002) and at Caravaca, Spain (Kaiho et al., 1999). The gradual decrease in the K/SM ratio in Zone P1a (1) suggests a rising sea level and change to a warmer and drier climate.

4.3. Trace elements

All trace element concentrations in the bulk samples show distinct increases at the K–T boundary from: 800 to 2000 ppm Sr, 20 to 55 ppm Rb, 60 to 350 ppm Zn, 65 to 300 ppm Zr and 60 to 400 ppm Ba (Fig. 3A). Arsenic, Zn, Cu and Ni indicate biomass constituents (Knauer and Martin, 1982), whereas Zr and Rb reflect the clay or detrital fraction whereas Ba and Sr show a hybrid behaviour which is controlled as well by biogenic activity as by the accumulation of clayey and detrital sediments (Murray and Leinen, 1996; Schroeder et al., 1997). Calcium and Sr concentrations do not correlate well (Fig. 3A) which is due to the incorporation of Sr in the carbonate phase as well as in the clay and feldspar fraction. The K–T shift in trace element concentration is negatively correlated with calcite content (CaO) which reflects the lithological change to carbonate-poor sediments during the early Danian. However, these values have to be evaluated within the context of the highly variable sediment accumulation rates across the K–T transition. Sediment accumulation rates average 3 cm/1000 yr for Zone CF1, 1 cm/1000 yr for Zone P0 and 2.25 cm/1000 yr for Zone P1a. For the thin K–T boundary clay and red layer, the sediment accumulation rate may be as low as 0.1 cm/1000 yr. If these sedimentation rates are taken into consid-

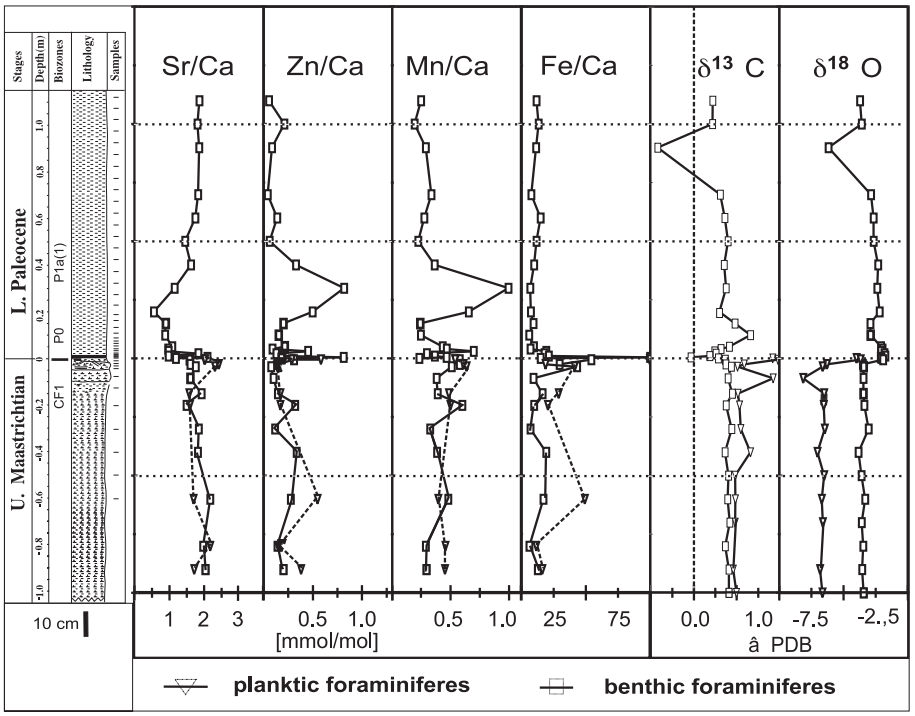

Fig. 4. Variations of Sr/Ca, Zn/Ca, Mn/Ca, Fe/Ca ratios and $\delta^{13}C$ and $\delta^{18}O$ values in foraminifera from 1 m above to 1 m below the K–T boundary at the Elles II section.

eration, it is obvious that at least a part of the trace element peaks observed at the K–T boundary are due to this condensed sedimentation. To account for the different sedimentation rates, the element fluxes to the sediment (Fig. 3B) were calculated using the sedimentation rates above. Sediment densities were assumed to average at 2.4 g/cm^3 for silicates, 3 g/cm^3 for carbonates and 4.5 g/cm^3 for iron oxides and hydroxides. Thus the sediment density was calculated as:

$$\rho_{sed} = 2.4\times(1-(CaCO_3 + Fe_2O_3))+$$

$$3\times CaCO_3 + 4.5\times Fe_2O_3\ [g/cm^3]$$

Within CF1, up to 10 cm below the K–T, flux and concentrations of nutrient type (e.g. Cu, Zn, Ba) and terrigenous elements (e.g. Rb, Zr) remained relatively constant with a slight minimum at approximately 80 cm below the K–T. Approximately 10 cm below the K–T the flux of nutrient type elements, as well as of the terrigenous elements, rapidly decreased. These trends are also observed in the carbonate-normalised biogenic fraction of the nutrient-type elements. Only CaO displays a slightly increased flux. Besides scattered values around the red layers, which may be induced by rapidly changing, but low sedimentation rates, the trend observed in the uppermost Maastrichtian continued at the base of P0. Within P0 the elemental flux remained approximately constant at a low level compared to the Maastrichtian. At 50 cm above the K–T the elemental flux increased rapidly for Cu, Zn, Rb, Zr and Ba to pre-K–T values, whereas Ca and Sr fluxes increased gradually but remained at comparably low levels.

This rapid decrease of the elemental flux within the uppermost Maastrichtian coincided with the maximum flooding period postulated from the clay mineralogy, and was followed by a period of steady high sea level with reduced elemental flux (nutrient type) and terrigenous elements within zone P0. The gradually rising sea level during

the sedimentation of P1a (1) was accompanied by a gradually increasing flux of Ca, Zn and Zr, partially of Cu, Sr and Ba, and by decreasing Rb. This pattern reflects gradually increasing productivity of planktic carbonate and detrital terrigenous flux. For the samples of the Maastrichtian succession an estimate of the biogenic fraction (excess values) of the nutrient and hybrid type elements was calculated similar to Murray and Leinen (1996), by using a practically carbonate-free sample of the section as a proxy for the chemical composition of the local detrital source. Titanium and Zr were used as conservative detrital elements. For the Palaeocene succession no estimate of the biogenic fraction of the nutrient-type elements could be calculated due to the very low carbonate content of these sediments. The excess values for the Elles II sections are generally low. Nevertheless, the excess ratios reflect the same general trends as the bulk compositions.

Trace element compositions of foraminifera normalised to Ca show significant variations at the K–T boundary for all elements and near the P0–P1a boundary for Zn and Mn (Fig. 4). The element/Ca ratios range from 1580 to 2700 μmol/mol for Sr, 380 to 1250 μmol/mol for Mn, and 56 to 1050 μmol/mol for Zn. The observed ratios for Mn and Zn are considerable higher than those published by Boyle (1981), whereas the Sr/Ca ratios are at the same level as described by Rosenthal et al. (1997b). Since Zn/Ca and Mn/Ca ratios in foraminifera are very sensitive to contamination (e.g. surface coating of tests), this could explain the higher concentrations at the K–T and P0–P1a intervals as compared with published ratios. Similarly, the high Fe/Ca ratios at the K–T layer may be due to contamination of foraminiferal tests within the Fe-rich red layer. In addition, the increase in Mn/Ca and Zn/Ca of foraminifera at the K–T boundary layer is probably due to diagenetic effects. However, higher concentrations in trace metals at the K–T boundary at Elles, except for nutrient-type elements, can also be explained by a low biogenic sedimentation rate and almost constant detrital input. Apart from the anomalously high ratios at the K–T boundary and upper Zone P0, Zn/Ca, Mn/Ca and Fe/Ca are remarkably stable and similar below and above the K–T boundary, with no major trace element changes apparent within the upper part of CF1 and P0–P1a interval.

Strontium in foraminiferal tests shows no correlation to bulk concentrations. Within the uppermost Maastrichtian Sr/Ca ratios decrease gradually from 2170 μmol/mol to 1950 μmol/mol. In the interval from 1 to 5 cm below the K–T boundary Sr/Ca fluctuates between 1960 and 2270 μmol/mol. Just above the K–T boundary Sr/Ca ratios decrease to 1730 μmol/mol. Except for one sample at 18 cm which shows the lowest Sr/Ca ratios (1580 μmol/mol), Sr/Ca ratios increase gradually from 1730 μmol/mol at the K–T boundary to approximately 2000 μmol/mol near the top of Zone P0 and remained nearly constant within Zone P1a (1).

The Sr/Ca ratio within the uppermost metre of the Maastrichtian reflects the postulated sea level low inferred from clay mineralogy followed by a rising sea level and maximum flooding (Fig. 4). The apparent minimum in the Sr/Ca ratio at 18 cm in P0 coincided with the lowest carbonate content of the sediment and may be the result of recrystallisation of aragonite to calcite, or it may be of terrigenous origin. Above P0 the gradually increasing Sr/Ca values indicate a rising sea level as also observed by mineralogical data (K/SM ratio, Fig. 2B). The Sr residence time of approximately 100 kyr (Schlanger, 1988; Stoll and Schrag, 1996) may have attenuated the variation of Sr/Ca ratios in response to short-term sea level variations.

4.4. Factor analysis

Complex interaction of different processes like diagenesis, weathering, detrital input, and variable conditions of sedimentation strongly overprinted primary palaeoceanographic signals so that the interpretation of different palaeoproxies is not always straightforward. By applying factor analysis to the complex set of different proxy parameters, an attempt was made for a qualitative discrimination between post-depositional processes and palaeoceanographic trends.

Factor analysis was applied to bulk chemical compositions and mineralogical data. Since the

data could not be assumed to be normally distributed, the parameter-free Spearman rank correlation was used instead of the Pearson correlation matrix. The anomalous sample of the red layer was excluded from the factor analysis. Factors were extracted for the total section, and separately for parts above and below the K–T boundary. Factor loadings for trace elements and minerals in bulk samples for the total profile (data set 1), as well as separately for the profile below (data set 2) and above the K–T boundary (data set 3) are shown in Table 2 and are graphically represented in Fig. 5.

(1) In all three data sets, factor 1 generally reflects the opposite trend between the detrital continental input and biogenic/authigenic sedimentation, with high positive loadings for elements typically bound in minerals of terrigenous origin (TiO_2, Ga, Rb, Zr), and high negative loadings for the carbonate component (Ca). Because of the striking difference between the nature of sedimentation below and above the K–T boundary, factor 1 explains the highest share of the variance (51%) in data set 1, which includes all the samples. In addition to the associations common for all three of the first factors (F1s), in the total sample set factor 1 includes some other elements which also belong to the siliciclastic fraction (clay and feldspar), such as Nb, rare earth elements, and the part of Fe, Ba and heavy metals bound to the detrital fraction. Although Sr shows a low communality, it still has a moderately high negative loading on F1 (−0.40), pointing to its general association with the carbonate fraction. Conse-

Table 2
Principal component analysis from Spearman rank correlation matrix for bulk samples: Varimax rotated factor loadings (italics: 0.5–0.6; bold >0.6)

	Total			Upper			Lower		
	1	2	3	1	2	3	1	2	3
CaO	**−0.92**	0.19	0.10	**−0.78**	−0.11	*0.51*	−0.54	0.00	−0.03
TiO_2	**0.94**	−0.07	0.09	*0.50*	−0.45	−0.27	**0.78**	0.45	0.20
MnO	−0.39	**0.63**	0.30	**−0.94**	−0.14	0.02	0.20	**0.67**	0.05
Fe_2O_3	**0.80**	0.46	0.12	**−0.92**	−0.24	−0.05	*0.52*	**0.73**	0.16
Ni	**0.81**	−0.04	0.19	**0.75**	−0.17	0.20	0.29	**0.78**	0.21
Cu	**0.79**	−0.29	0.28	**0.70**	−0.38	−0.29	**0.67**	0.32	−0.10
Zn	**0.87**	0.04	0.06	0.17	*−0.55*	0.13	*0.52*	0.28	0.35
As	**0.77**	−0.03	0.45	0.29	**−0.76**	−0.15	0.13	**0.71**	0.05
Br	**0.91**	−0.12	−0.07	**0.68**	0.02	**−0.65**	0.07	−0.12	0.46
Rb	**0.91**	−0.29	−0.04	**0.82**	−0.26	−0.31	**0.63**	*-0.54*	0.27
Sr	−0.40	−0.43	0.25	0.24	**−0.61**	0.73	−0.08	**−0.65**	0.31
Y	**0.63**	0.63	0.07	**−0.87**	−0.09	−0.19	0.24	**0.61**	*0.59*
Zr	**0.93**	−0.23	0.04	**0.84**	−0.36	0.18	**0.79**	−0.04	*0.52*
Nb	**0.88**	0.04	−0.23	0.23	**0.71**	0.05	**0.76**	0.21	0.00
Cd	0.07	−0.36	0.07	0.46	0.09	0.02	0.29	−0.33	**0.60**
Sb	0.04	0.10	0.04	0.04	0.37	0.10	0.17	0.42	−0.17
Ba	**0.89**	−0.18	0.06	*0.53*	−0.58	0.43	**0.61**	−0.11	0.43
La	**0.88**	0.13	−0.09	0.21	*0.59*	−0.36	−0.15	0.25	**0.84**
Ce	**0.91**	0.23	0.10	−0.16	−0.03	**−0.89**	0.36	0.45	**0.70**
Pb	**0.84**	−0.15	−0.36	**0.60**	0.62	0.25	0.25	**−0.65**	−0.04
Ga	**0.95**	−0.15	0.01	**0.75**	−0.25	−0.38	**0.73**	0.28	0.19
Smectite	−0.05	**0.82**	−0.21	**−0.78**	0.24	0.20	**−0.72**	−0.01	0.38
Mica	0.15	*-0.50*	0.58	0.44	−0.42	−0.11	*0.57*	0.15	*0.59*
Kaolinite	0.05	**−0.81**	−0.30	**0.89**	0.01	0.10	0.48	−0.45	*-0.57*
Chlorite	−0.04	0.12	**0.80**	0.04	−0.21	*-0.54*	−0.00	**0.74**	0.38
Goethite	**0.82**	0.25	0.01	**−0.63**	−0.35	−0.27			
Jarosite.	0.30	**−0.61**	0.14	0.53	−0.25	0.25			
Expl. variance	13.78	3.77	1.87	10.24	4.15	3.44	6.00	5.47	4.04
Rel. variance	51.0%	14%	6.9%	37.9%	15.3%	12.7%	24.%	21.9%	16.2%

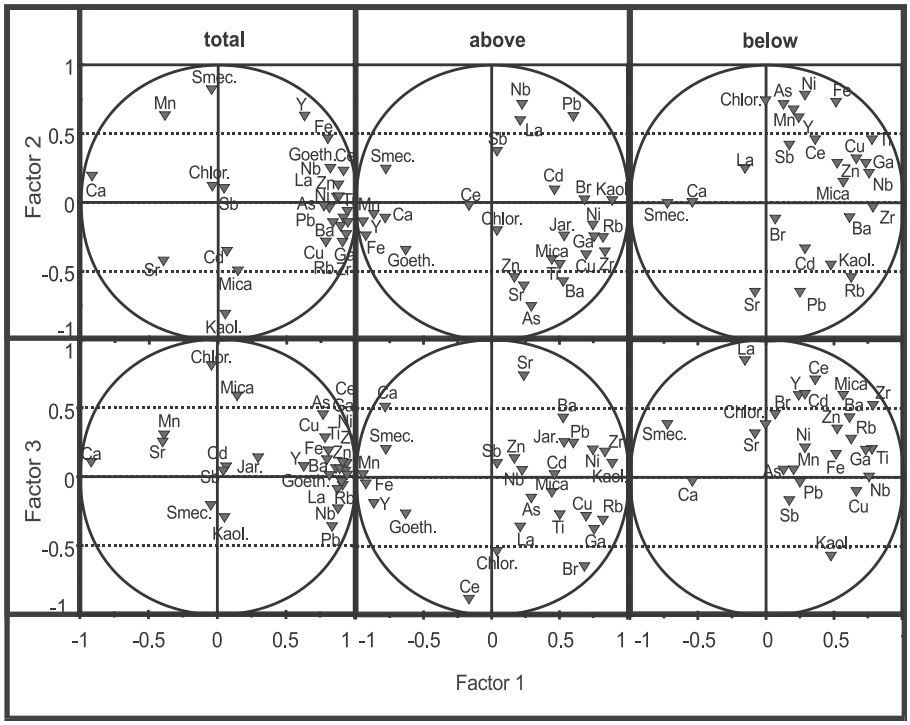

Fig. 5. Factor analysis. Plots of the first three factors extracted by principal component analysis from Spearman rank correlation matrix of the Elles II bulk samples for the total section, and separately for the intervals above and below the K–T boundary.

quently for the total profile, factor 1 mainly reflects the oceanographic differences between the parts below and above the K–T, with relatively high productivity of planktic carbonate and low terrigenous input below the K–T boundary and reduced productivity and higher detrital fluxes above it.

For the total profile factor 2 shows high positive loadings for MnO, (Fe_2O_3) and smectite and high negative loadings for kaolinite (Fig. 5). Since no mafic rocks are present in this part of the African margin, smectite is of detrital origin and primarily from eroded continental soils. Therefore, the association of smectite and kaolinite with opposite signs in factor 2 may be interpreted as climatic changes reflecting humid/warm to dry and seasonal variations with sea level fluctuations. Factor 3 shows highest loadings for chlorite and mica, and indicates low hydrolysis weathering, typical of cool to temperate and/or dry climates.

(2) In the carbonate-dominated portion of the profile below the K–T boundary (data set 2), factor 1 again reflects the contrary relationship between terrigenous (TiO_2, Rb, Zr, Nb, Ba, Ga) and biogenic (CaO) sedimentation, although the loading for CaO is only moderately low, and the variance explained by this factor is only 24%. The lack of covariance between Sr and Ca indicates that on the shelf and upper bathyal environment, a part of the Sr is of terrigenous origin, even in carbonate-rich sediments. In carbonates of biogenic origin, variations in the Sr/Ca ratio reflect variations of the Sr content of the palaeo-seawater, which is probably a consequence of Sr released due to aragonite weathering induced by sea level changes (Stoll and Schrag, 1996, 1998). In bulk sediments of the shelf areas this effect will be overprinted by the Sr input of terrigenous origin.

Factor 2 has high loadings for the elements Mn, Fe, Ni and As. Ni and As are typically coprecipitated with, or adsorbed, on Fe-oxyhydrates. Nevertheless, the equally high loading of chlorite may hint at an association of these ele-

ments with Fe-rich chlorite. Negative loadings for Rb, Sr and Pb, with no correlation to Ca, indicate that a part of Sr in the carbonate-rich marls below the K–T boundary was released by weathering of feldspars.

Factor 3 shows high positive loadings for rare earth elements (La, Ce, Y) and mica, and negative loadings for kaolinite. This possibly reflects the trend to less humid climates during the latest Maastrichtian, which modified the products of terrigenous weathering.

(3) Within the grey clayey shales above the K–T boundary (data set 3), factor 1 includes the mineral/element association corresponding to factor 2 of data set 1, based on the total profile (high positive loadings for kaolinite, less for mica and negative loadings for smectite and the elements Mn and Fe). If factor 2 of data set 1 (total profile) is interpreted to express sea level fluctuations, it would follow that in this part of the sedimentary sequence, periods of increased carbonate sedimentation were coupled with transgressive episodes. In other words, the gradual transition from drier conditions and a low sea level at the top of Zone P0 towards a rising sea level and a warmer climate within P1a was accompanied by decreased detrital mineral flux, increased carbonate sedimentation rates (Keller and Stinnesbeck, 1996), and higher Fe and Mn fixation in the sediments.

Factors 2 and 3 of data set 3 (samples above the K–T boundary) include the elements Sr and Ba (in F2 also As) with identical signs. This suggests two different mineralogical sources for these elements in the Danian sequence. In factor 2 the loading of CaO is very low, and indicates that a part of Sr, together with Ba and As, is bound to the clay fraction. Thus, in sediments with low carbonate contents, a considerable part of Sr is likely to be of terrigenous origin. On the other hand, in factor 3 both Sr and CaO are relatively high, representing the part of Sr of biogenic origin bound to the carbonate fraction.

The relatively high loadings with reversed signs of some other elements (like Nb and Pb in F2 and Br and Ce in F3) cannot be readily interpreted; they may also represent statistical artifacts. The continental input is accompanied by alteration of feldspars, which frees elements like Pb, but also detrital material that is characterised by Nb. The separation of Nb from Zr (included in F1) may hint at two different sources of terrigenous material, of which one is probably more connected to the diffuse flux of terrigenous dust and the second to a local source.

4.5. Stable isotopes

4.5.1. Role of diagenesis

Diagenetic overprint and vital effects can alter primary palaeoceanographic signals, thus complicating the interpretation of the C and O isotope ratios (e.g. Zachos et al., 1989; Jenkyns et al., 1994; Mitchell et al., 1997). Due to the higher ratio of oxygen in pore waters to oxygen in carbonate as compared to the similar ratio of carbon, oxygen isotopes are far more sensitive to post-depositional changes. Lithologies like clays and marls, having low porosities, are relatively closed to the circulation of water and are less subject to diagenesis than limestones and chalks (Mitchell et al., 1997). Paul et al. (1999) showed that differential cementation between chalk and marl facies may produce oscillations in phase with the lithology, overprinting and smoothing out the primary oceanographic isotopic record. The morphology of the foraminifera (shape, number and dimension of chambers) can also control the amount of chamber infilling, but individual foraminiferal species generally show fewer diagenetic effects, unless massive recrystallisation occurs, or the percentage of cement is large (Mitchell et al., 1997).

Beside physical evidence of diagenetic alteration, which is readily detected by microscopic investigation of foraminiferal specimens and polished thin sections (e.g. cement overgrowth, infillings of pores or foraminiferal chambers, dissolution or recrystallisation features), a covariance of $\delta^{18}O$ and $\delta^{13}C$ values is often used as a geochemical criterion to identify and quantify the influence of diagenesis on primary isotopic signatures (Jenkyns et al., 1995; Jenkyns, 1996; Mitchell et al., 1997). According to these authors, the covariance is due to mixing of variable quantities of isotopically lighter cement of diagenetic origin with primary skeletal carbonate, so that the

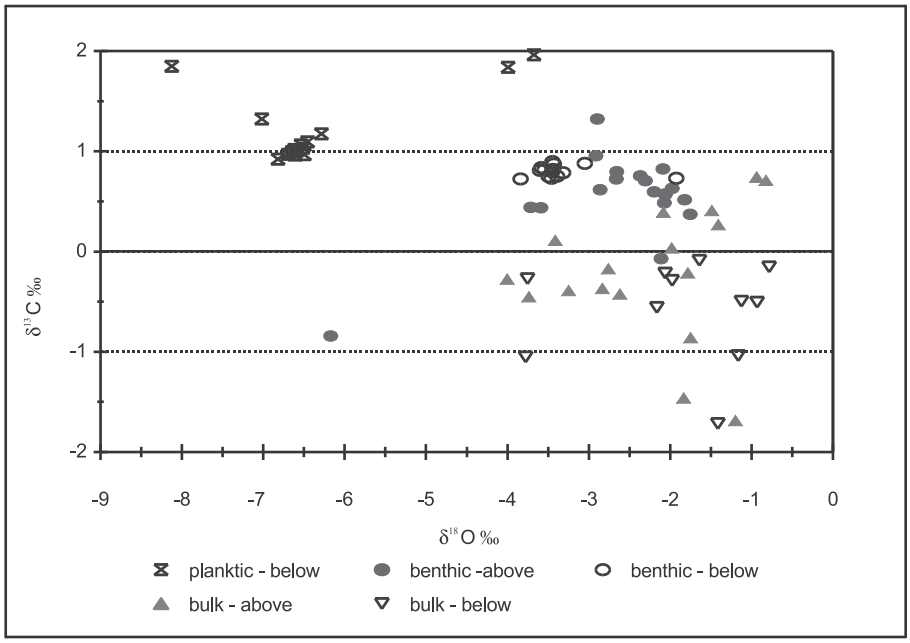

Fig. 6. Cross-plot of the $\delta^{13}C$ and $\delta^{18}O$ values of the analysed samples.

position of a sample on the mixing line will depend on the proportion of cement in the sample. However, the covariation of carbon and oxygen in planktic foraminifera can also be related to changes in the carbonate concentration of seawater (Spero et al., 1997; Bijma et al., 1999).

A cross-plot of the $\delta^{18}O$ and $\delta^{13}C$ values of the foraminifera and bulk samples investigated does not suggest mixing trends in any of the populations considered (Fig. 6). Thus, only minor effects of contamination by diagenetic cement and recrystallisation can be expected. The microscopic inspection of the material used for the isotopic analyses showed that (probably due to the clayey–marly matrix) individual specimens of foraminiferal tests are well preserved, generally without visible signs of carbonate dissolution or recrystallisation and calcite overgrowth. The stratigraphic reproducibility of the isotopic signals also supports the preservation of the primary oceanographic information (see below). Nevertheless, diagenetic effects cannot be ruled out in some samples (e.g. 90 cm above the K–T boundary) where both $\delta^{18}O$ and $\delta^{13}C$ values show marked negative excursions.

4.5.2. $\delta^{13}C$ values of benthic foraminifera

$\delta^{13}C$ values of benthic foraminifera in Maastrichtian marls are very stable ranging between 0.8 and 0.7‰. Similar values are also seen for the most part above the K–T boundary (Fig. 7). Exceptions occur at the red layer, where $\delta^{13}C$ values decreased to −0.07‰ followed by a short-term increase to 0.5‰ in the first 10 cm of the boundary clay, and a return to decreased stable, pre-K–T values 20 cm above the K–T boundary. $\delta^{13}C$ values of the Maastrichtian surface dweller *Rugoglobigerina rugosa* are nearly the same as for the benthic species (*Cibicidoides pseudoacuta*) between 100 and 50 cm below the K–T boundary and reflect the absence of a surface-to-deep carbon gradient in a shallow water environment. In the last 50 cm of the Maastrichtian the presence of a minor $\delta^{13}C$ gradient reflects changes in primary productivity. Note that the single point excursion within the bioclastic layer is likely due to the presence of reworked species. At the K–T boundary, planktic values increased by 0.9‰, in contrast to the decreased benthic values. This may indicate that *R. rugosa* tests analysed from the boundary at Elles are reworked. However, a sim-

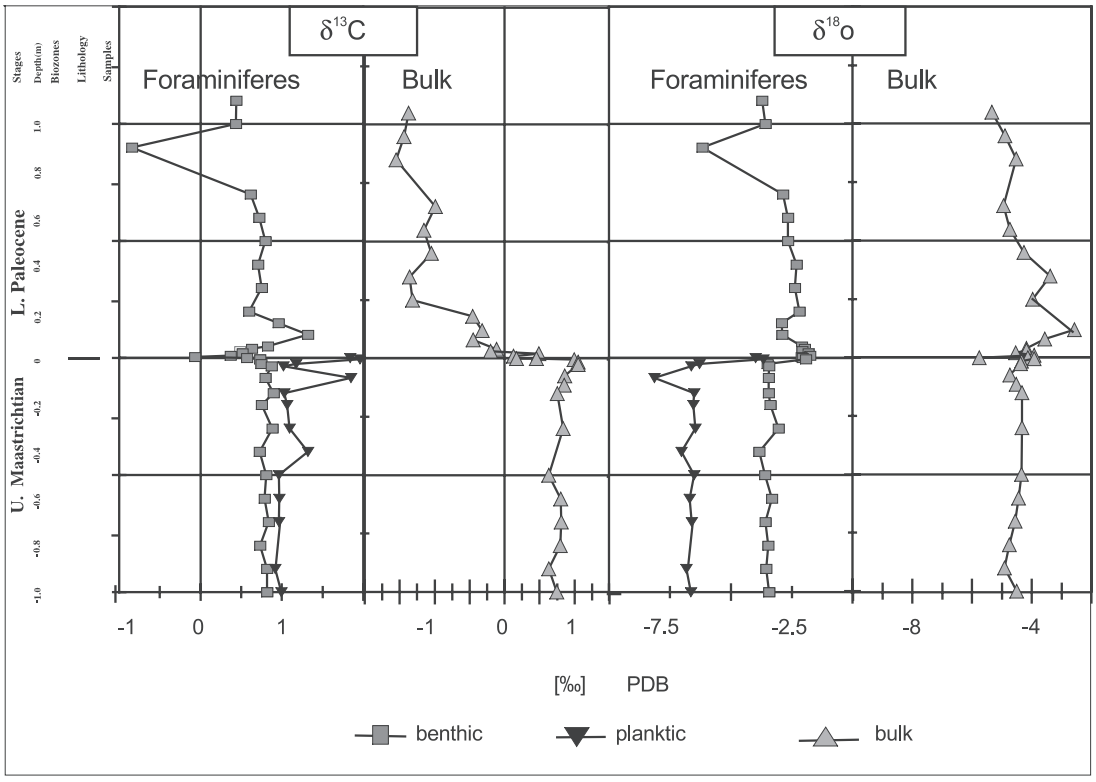

Fig. 7. Comparison of the $\delta^{13}C$ and $\delta^{18}O$ profiles of benthic and planktic foraminifera and bulk rock samples from 1 m above to 1 m below the K–T boundary at Elles II.

ilar increase in $\delta^{13}C$ values of *R. rugosa* in the uppermost 5–10 cm of the Maastrichtian was previously also observed at Stevns Klint and Nye Kløv in Denmark (Schmitz et al., 1992; Keller et al., 1993), which argues against this interpretation. Hence, this increase may reflect increased surface productivity just before the K–T boundary event. At El Kef, the planktic foraminifer *Pseudotextularia deformis* was analysed and, in contrast to *R. rugosa*, shows a decrease at this time. However, the different $\delta^{13}C$ signals in *R. rugosa* and *P. deformis* may reflect their relative positions in the water column, with *R. rugosa* reflecting changes closer to the ocean surface.

Carbon isotope data of single species indicate relatively stable bioproductivity during the latest Maastrichtian at Elles. This interpretation is consistent with results from other K–T boundary sections (Zachos and Arthur, 1986; Keller and Lindinger, 1989; Zachos et al., 1989). The consistently heavier planktic $\delta^{13}C$ values, as compared with benthic values, indicate a vertical carbon isotope gradient with high surface water bioproductivity. The temporary negative $\delta^{13}C$ excursion in benthic species, which began just below the K–T boundary, implies a temporary decrease in bioproductivity which coincided with an increase in trace metals contents (Figs. 3 and 6).

At Elles, drastically reduced carbonate accumulation rates began at the K–T boundary and continued through Zone P1a (Fig. 2A), indicating a lengthy period of reduced surface water productivity. Zachos and Arthur (1986) estimated that carbonate accumulation rates in the deep sea remained depressed for at least 1–2 Myr, though Keller and Lindinger (1989) estimated that recovery to pre-K–T values began about 0.5 Myr after the K–T boundary event and a gradual increase in carbonate deposition began already in Zone P1a (just after 0.2 Myr). Our data support a pro-

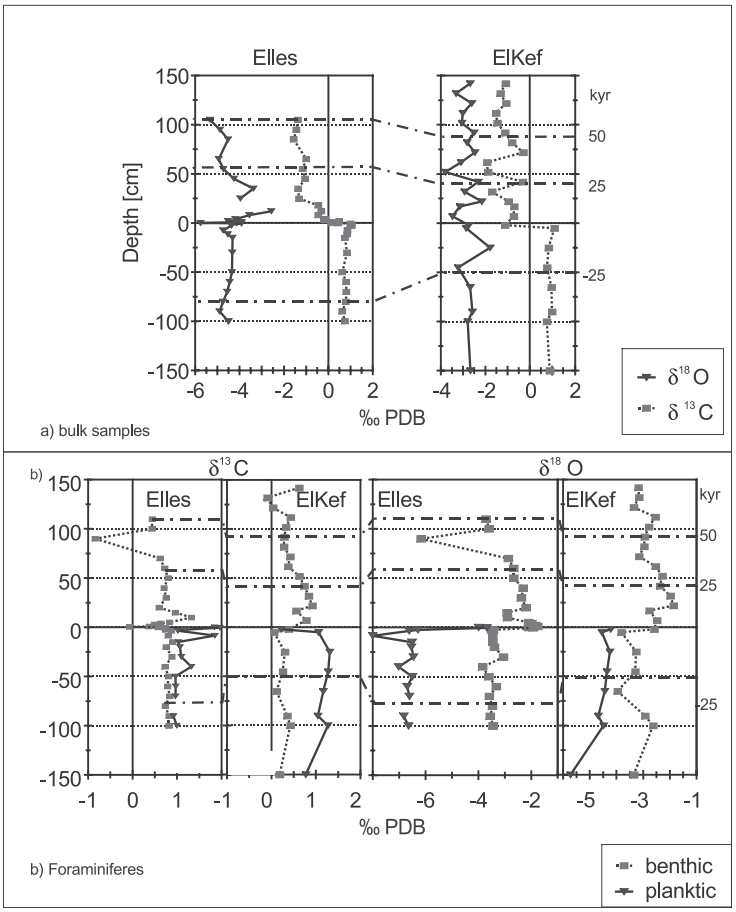

Fig. 8. Comparison of $\delta^{13}C$ and $\delta^{18}O$ profiles of the Elles II and El Kef K–T sections. Data from El Kef are from Keller and Lindinger (1989).

longed depressed carbonate accumulation rate through Zone P1a, but also indicate that an albeit slow recovery started in zone P0 as implied by the slowly increasing CaO content (Fig. 2A).

The strong negative shift in bulk $\delta^{13}C$ observed globally across the K–T boundary in low to middle latitude sediments was also observed in benthic foraminifera at Elles (Fig. 7). However, unlike at El Kef or other deeper marine sections where $\delta^{13}C$ values of benthic foraminifera show no significant variation at the K–T boundary, at Elles they show a brief negative excursion of nearly 2‰ (Fig. 7). Since the Elles section was deposited in a shallower middle neritic environment (100–200 m), we assume that bottom and surface waters were similarly affected by decreased primary productivity. This interpretation is supported by the similar parallel decreased primary productivity across the K–T boundary in the shallow water environments of Nye Kløv and Brazos River sections (Barrera and Keller, 1990; Keller et al., 1993).

$\delta^{18}O$ values of uppermost Maastrichtian benthic and planktic foraminifera are also relatively stable, averaging −3.4‰ for benthics and −7‰ for planktics, respectively. There is a single point negative excursion in planktic foraminifera within the bioclastic layer, which is probably an artifact of reworked species. Just below the K–T boundary benthic and planktic values increased by 1.5‰ and 3.0‰ respectively. In the first 70 cm above the K–T boundary, benthic values

range between −2.3 and −2.8‰, and about 0.7‰ more positive than the K–T boundary (Fig. 7), indicating cooler temperatures. Below the K–T boundary, benthic and planktic values are well separated and reflect the temperature difference between surface and bottom waters. At the K–T boundary within the red and green clay layers the $\delta^{18}O$ values of benthics increased to −1.5‰ and remained only 1.9‰ higher than those of the planktic foraminifera.

$\delta^{18}O$ measurements of planktic and benthic foraminifera and bulk rock indicate climatic trends associated with sea level changes and the K–T boundary event. Because foraminiferal species at Elles may be partly recrystallised, they may not represent original $\delta^{18}O$ values and therefore no absolute temperature changes can be calculated. However, the long-term trends suggest a brief cooling at the K–T boundary in benthic and planktic foraminifera followed by nearly pre-K–T bottom water temperatures in Zones P0 and P1a (1) (Fig. 7). Alternatively, these $\delta^{18}O$ variations may be partly influenced by salinity fluctuations. Similarly cooler temperatures during the K–T and earliest Danian are observed at El Kef (Keller and Lindinger, 1989; Keller et al., 1996). Significantly cooler early Danian climatic conditions are generally recorded for deep water sites (Zachos and Arthur, 1986; Stott and Kennett, 1990). In the shallower water (sub-photoic zone) Danish continental shelf sections at Nye Kløv and Stevns Klint, benthic and planktic $\delta^{18}O$ values record a temporary cooling beginning just below the K–T boundary and continuing into the early Danian P0 Zone (Keller et al., 1993), though at the shallower water section at Brazos River, Texas, $\delta^{18}O$ values are 2–3‰ lighter in the lower Danian P0 and P1a Zones, suggesting strong salinity fluctuations (Barrera and Keller, 1990).

Comparison of the $\delta^{13}C$ and $\delta^{18}O$ profiles of the Elles and El Kef sections shows similarities and differences related to their respective environments (Fig. 8). $\delta^{13}C$ values of bulk samples, benthic and planktic species are similar for the uppermost Maastrichtian. As expected there is a greater surface-to-deep $\delta^{13}C$ gradient at El Kef than at Elles due to the greater water depth at El Kef. However, the higher surface-to-deep $\delta^{18}O$ gradient at Elles is not easily explained and may be due to salinity effects in this shallower water section. At both sections, a 2–3‰ shift to lighter $\delta^{13}C$ values occurred at the K–T boundary, though not in benthic foraminifera at El Kef. The global decrease in $\delta^{13}C$ of surface waters is generally interpreted as resulting from a sudden reduction in oceanic primary productivity. At Elles and El Kef primary productivity remained low throughout the lower Danian Zone P1a and recovery occurred within Zone P1b–c (Keller and Lindinger, 1989). Such prolonged low primary productivity is generally observed in low to middle latitude deep sea sequences, but not at higher latitudes where the $\delta^{13}C$ shift is much reduced or absent and primary productivity remained relatively high even within the early Danian (Barrera and Keller, 1990; Keller et al., 1993; Pardo et al., 1996; Oberhänsli et al., 1998; Pardo et al., 1999). However, in many deep sea sections recovery seems to have occurred almost immediately after the K–T boundary. This appears to be an artifact of an incomplete record where Zone P0 is most often missing and Zone P1a is highly condensed (Perch-Nielsen et al., 1982; MacLeod and Keller, 1991).

5. Discussion

Palaeoclimatic changes are generally related to sea level fluctuation as well as weathering and erosion (Schlanger, 1988; Hallam, 1992). The changes in lithology, clay mineralogy, trace element and isotope geochemistry of sediments and microorganisms, such as planktic and benthic foraminifera, are useful proxies to evaluate environmental changes. Our studies of the relatively shallow water K–T boundary transition at Elles II reflect environmental conditions before, during and after the K–T boundary on a continental shelf in proximity to North Africa. Through most of Tunisia, the K–T boundary transition is unusually complete with high sedimentation rates in several outcrops at El Kef, Ain Settara, El Melah and Elles (Keller et al., 1998). Among these four localities, the section at Elles II has

the highest sedimentation rate and appears the most complete. Based on our high resolution geochemical and mineralogical analysis of this section, the following scenario can be suggested.

A general increase in detrital influx (bulk mineralogy, clay minerals, Ti, Zr, Nb) indicates an overall long-term change in climate, beginning in the uppermost Maastrichtian Zone CF1 that continued into the lower Danian, and culminated near the K–T boundary, accompanied by a major change in weathering rates and by sea level fluctuations (characteristic K/SM ratio, Sr/Ca ratios in benthic foraminifera). About 1 m below, or about 33 kyr prior to the K–T boundary event, equable warm climatic conditions prevailed as indicated by oxygen isotopes and clay minerals (Figs. 2B and 6). High though variable kaolinite content, slightly increased Zr concentrations in bulk samples and increased Sr/Ca ratios in benthic foraminifera suggest that a climatic change to more humid conditions accompanied by accelerated runoff and possibly a lower sea level could have occurred 60 cm (about 20 kyr) below the K–T boundary.

Within the last 60 cm (20 kyr) of the Maastrichtian, surface and bottom water temperatures remained relatively warm, suggested by the $\delta^{18}O$, but a distinct surface-to-deep $\delta^{13}C$ gradient was established, suggesting increased surface productivity. A few thousand years before the K–T boundary (5–10 cm below K–T), a sea level transgression accompanied by high humidity is marked by a foraminiferal packstone, a rise in kaolinite, mica, chlorite (Fig. 2B) and decreasing Sr/Ca ratios in benthic foraminifera (Fig. 4). This transgressive event was also accompanied by significant reworking as suggested by the increase in clay minerals from different sources and fluctuations of isotope and trace element values in monospecific foraminifera (Figs. 2B, 4 and 6). Increased smectite suggests that the sea level transgression was accompanied by less humid climatic conditions.

It is suggested that the sea level reached maximum height at the K–T boundary (red layer) and the base of Danian (base of P0) amid drier climates as marked by peak abundance in smectite and low Sr/Ca ratios in benthic foraminifera. Bulk rock and benthic foraminiferal $\delta^{18}O$ values suggest somewhat cooler bottom and surface water temperatures at this time at both Elles II and El Kef (Figs. 6 and 7). The maximum flooding surface (MSF, Fig. 2B) coincided with the onset of rapidly declining bulk and fine fraction $\delta^{13}C$ values at Elles II and El Kef and a reduced Ca, Cu, Zn and Sr flux to the sediment and marked a very rapid drop in surface productivity of planktic carbonate. At the same time, total organic carbon (TOC) peaked (in the red layer) probably as a result of several processes (Adatte et al., 2002), including changes in marine and/or terrestrial productivity, sedimentation rates, or low oxygen conditions at the sediment–water interface. This dramatic change also coincided with the mass extinction of tropical and subtropical planktic foraminifera, the major terminal decline in the abundance of generalist survivor species and the sudden rise to dominance of opportunistic species (e.g. *Guembelitria*: Keller et al., 1996, 2002). The presence of an Ir anomaly, Ni-rich spinels and spherules within the red layer (Rocchia et al., 2002) indicates that an impact event coincided with the maximum flooding, exacerbating the already stressed environmental conditions and possibly causing the mass extinction in planktic foraminifera.

As indicated by the high K/SM ratio in the sediment and increasing Sr/Ca ratios in benthic foraminifera sea level may have remained high and humidity seems to have increased within the lower Danian Zone P0, though both gradually decreased towards the top of P0 (Figs. 2B and 4). $\delta^{13}C$ values reached minima at both Elles II and El Kef near the top of P0 and remained low in Zone P1a (Figs. 6 and 7), whereas surface temperatures may have remained relatively cool. In the upper part of Zone P0, a sea level lowstand is indicated by high kaolinite, reflecting accelerated terrigenous runoff amid increasingly humid conditions (Fig. 2B). Above this interval, in the lower part of Zone P1a (1), sea level gradually rose as suggested by increased smectite and decreased kaolinite. Oxygen isotopes suggest that climate returned to nearly pre-K–T conditions near the top of Zone P1a, though surface productivity remained depressed. Planktic foraminifera began their recovery with the evolution of more

diverse early Tertiary assemblages within Zone P1a accompanied by a rising sea level and increased carbonate sedimentation. The sea level fluctuations interpreted from the Elles II succession have been observed in sections worldwide and indicate global eustatic changes (Donovan et al., 1988; MacLeod and Keller, 199l; Keller and Stinnesbeck, 1996).

6. Conclusions

(1) Decreasing Sr/Ca ratios in foraminifera and variations in the clay mineralogy (variable low K/SM ratios) indicate that the latest Maastrichtian (top 100 cm, about 33 kyr) in Tunisia was marked by a relatively warm but humid climate and a rising sea level.

(2) Our data suggest that the K–T boundary at Elles II coincided with: (a) a maximum flooding event and with very low sediment accumulation rates (red layer and black boundary clay), (b) drier and possibly cooler climate, (c) rapidly decreasing surface productivity of planktic carbonate (lower $\delta^{13}C$ values, reduced flux of heavy metals to the sediment), (d) high TOC values related to a change in marine and terrestrial productivity and (e) an impact event (Ir anomaly, Ni-rich spinels, spherules; Rocchia et al., 2002). The coincidence of the impact event with ongoing climatic and sea level changes likely exacerbated the already highly stressed environmental conditions, leading to the mass extinction of tropical and subtropical planktic foraminifera.

(3) $\delta^{18}O$ values, clay minerals and Sr/Ca ratios in benthic foraminifera indicate that the lowermost Danian Zone P0 in Tunisia was marked by cooler temperatures (higher $\delta^{18}O$ values), generally high humidity and a higher sea level (clay minerals, low Sr/Ca ratios in benthic foraminifera). Near the top of P0, drier climatic conditions and a decreased sea level mark a lowstand which is commonly associated with erosion and a short hiatus (high K/SM ratio, increasing Sr/Ca ratios in benthic foraminifera). Within Zone P1a, sea level rose gradually (decreasing K/SM ratio), accompanied by a drier and warmer climate (decreasing higher $\delta^{18}O$ values, clay mineralogy).

Acknowledgements

This study was supported by the Deutsche Forschungsgemeinschaft (Grants Stu 169/10-1, 10-2 and Sti 128/2-1, 2-2), and the National Science Foundation (Grant INT 95-04309). We thank Markus Leosson for measuring the stable isotopes. The critical reviews of J. McManus, H.C. Jenkyns and S. Bains helped to improve the manuscript.

References

Adatte, T., Keller, G., Li, L., Stinnesbeck, W., 2002. Late Cretaceous to Early Palaeocene climate and sea-level fluctuations: The Tunisian record. Palaeogeogr. Palaeoclimatol. Palaeoecol. 178, 165–196.

Adatte, T., Rumley, G., 1989. Sedimentology and mineralogy of Valanginian and Hauterivian in the stratotypic region (Jura mountains, Switzerland). In: Wiedmann, J. (Ed.), Cretaceous of the Western Tethys. Proceedings 3rd International Cretaceous Symposium. Scheizerbart'sche Verlagsbuchhandlung, Stuttgart, pp. 329–351.

Adatte, T., Stinnesbeck, W., Keller, G., 1996. Lithostratigraphic and mineralogical correlations of near-K-T boundary clastic sediments in northeastern Mexico: Implications for mega-tsunami or sea-level changes? Geol. Soc. Am. Spec. Pap. 037, pp. 197–210.

Barrera, E., Keller, G., 1990. Stable isotope evidence for gradual environmental changes and species survivorship across the Cretaceous/Tertiary boundary. Paleoceanography 5, 867–890.

Ben Abdelkader, O., Zargouni, F., 1995. Biostratigraphy and lithology of the Cretaceous-Tertiary stratotype boundary of El Kef (Tunisia). Ann. Mines Géol. 35, 11–22.

Berggren, W.A., Kent, D.V., Swisher, C.C., Aubry, M.-P., 1995. A revised Cenozoic geochronology and chronostratigraphy. In: Berggren, W.A. et al. (Eds.), Time Scales and Global Stratigraphic Correlations. Soc. Econ. Paleontol. Mineral. Spec. Publ. 54, pp. 129–131.

Bijma, J., Spero, H.J., Lea, D.W., 1999. Reassessing foraminiferal stable isotope geochemistry: impact of the oceanic carbonate system (experimental results). In: Fischer, G., Wefer, G. (Eds.), Use of Proxies in Paleoceanography. Springer Verlag, Berlin, pp. 489–512.

Boyle, E.A., 1981. Cadmium, zinc, copper and barium in foraminiferea tests. Earth Planet. Sci. Lett. 53, 11–35.

Boyle, E.A., 1986. Paired carbon isotope and cadmium data from benthic foraminifera. Implications for changes in oceanic phosphorous, oceanic circulation, and atmospheric carbon dioxide. Geochim. Cosmochim. Acta 50, 265–276.

Brasier, M.D., 1995. Fossil indicators of nutrient levels. 1: Eutrophication and climate change. In: Bosence, D.W.J., Allison, P.A. (Eds.), Marine Palaeoenvironmental Analysis from Fossils. Geol. Soc. Spec. Publ. 83, pp. 113–132.

Brinkhuis, M., Zachariasse, W.J., 1988. Dinoflagelate cysts, sealevel changes and planktic foraminiferes across the Cretaceous-Tertiary boundary at El Maria, northwest Tunisia. Mar. Micropaleontol. 13, 153–191.

Broecker, W.S., Peng, T.S., 1984. The climate-chemistry connection. In: Hansen, J.E., Takahashi, T. (Eds.), Climate Sensitivity. Am. Geophys. Union Monogr. 29, pp. 327–336.

Burollet, P.F., 1956. Contributions à l'ètude stratigraphique de la Tunisie Centrale. Ann. Mines Géol. Tunis 18, 310 pp.

Burollet, P.F., 1967. General Geology of Tunisia. Petroleum Explor. Soc. Libya, 9th Annual Field Conference, Tripoli, pp. 51–58.

Cande, S.C., Kent, D.V., 1992. A new geomagnetic polarity time scale for the Late Cretaceous and Cenozoic. J. Geophys. Res. 97, 13917–13951.

Cande, S.C., Kent, D.V., 1995. Revised calibration of the geomagnetic polarity time scale for the Late Cretaceous and Cenozoic. J. Geophys. Res. 100, 6093–6095.

Chamley, H., 1989. Clay Sedimentology. Springer, Berlin.

Chamley, H., Deconinck, J.F., Millot, G., 1990. Sur l'abondance des minéraux smectitiques dans les sediments marins communs déposés lors des periodes de haut niveau marin du Jurassique supérieur au Paleogène. C.R. Acad. Sci. Se. 2, Méc, Phys. Chim. Sci. Univers Sci. Terre 311, 1529–1536.

Chamley, H., Masse, J.-P., 1975. Sur la signification des minèraux argileux dans les sèdiments barrèmiens et bèdouliens de Provence (SE de la France). 9ëme Congr. Int. Sèdimentol., Nice, Vol. 1, pp. 25–30

Debrabant, P., Fagel, N., Chamley, H., Deconinck, J.F., Rercourt, P., Trouillet, A., 1992. Clay sedimentology, mineralogy and chemistry of Mesozoic sediments drilled in the northern Paris Basin. Sci. Drill. 3, 138–152.

Deconinck, J.F., 1992. Sédimentologie des argiles dans le Jurassique-Crétacé du Europe occidentale et du Maroc. Mém. Thesis, Univ. Lille I, Lille.

Deconinck, J.F., Beaudoin, B., Chamley, H., Joseph, P., Raoult, J.-F., 1985. Contrôles tectonique, eustatique et climatique de la sédimentation argileuse du domaine subalpin francais au Malm-Crétacé. Rev. Géogr. Phys. Geol. Dyn. 26, 311–320.

Dittert, N., Baumann, K.-H., Bickert, T., Heinrich, R., Huber, R., Kinkel, H., Meggers, H., 1999. Carbonate dissolution in the deep-sea: methods, quantification and paleoceanographic application. In: Fischer, G., Wefer, G. (Eds.), Use of Proxies in Paleoceanography. Examples from South Atlantic. Springer, Berlin, pp. 255–284.

Donovan, A.D., Baum, G.R., Blechschmidt, G.L., Loutit, T.S., Pflum, C.E., Vail, P.R., 1988. Sequence stratigraphic setting of the Cretaceous-Tertiary boundary in Central Alabama. In: Berggren, W.A. et al. (Eds.), Sea Level Changes. Soc. Econ. Paleontol. Mineral. Spec. Publ. 42, pp. 299–307.

Donze, P., Colin, J.P., Damotte, R., Oertli, H.J., Peypouquet, J.P., Said, R., 1982. Les ostracodes du Campanien terminal à l'Eocène inférieur de la coupe du Kef, Tunisie nord-occidentale. Bull. Centres Rech. Explor. Prod. Elf-Aquitainne 6, 273–335.

Donze, P., Jardiné, S., Legoux, O., Masure, E., Méon, H., 1985. Les événements à la limite Crétacé-Tertiaire au Kef (Tunisie septentrionale) l'analyse palyno-planctologique montre qu'un changement climatique est décelable à la base du Danien. Actes du 1er Congrès nationale des Sciences de la Terre, Tunis, pp. 161–169

Dymond, J., Suess, E., Lyle, M., 1992. Barium in deep-sea sediments: A proxy for paleoproductivity. Paleoceanography 7, 163–181.

Epstein, S., Buchsbaum, H., Lowenstam, H., Urey, H.C., 1953. Revised carbonate-water isotopic temperature scale. Geol. Soc. Am. Bull. 64, 1315–1325.

Erez, J., Luz, B., 1992. Temperature control of oxygen-isotope fractionation of cultured planktic foraminifera. Nature 297, 220–222.

Fischer, G., Wefer, G. (Eds.), 1999. Use of Proxies in Paleoceanography – Examples from South Atlantic. Springer, Berlin.

Gaucher, G., 1981. Les Facteurs de la Pedogenèse. G. Lelotte, Dison, Belgium.

Gibbs, R.J., 1977. Clay mineral segregation in the marine environment. J. Sediment. Petrol. 47, 237–243.

Gingele, F.X., Zabel, M., Kasten, S., Bonn, W.J., Nürnberg, C.C., 1999. Biogenic barium as a proxy for paleoproductivity: Methods and limitations of application. In: Fischer, G., Wefer, G. (Eds.), Use of Proxies in Paleoceanography – Examples from South Atlantic. Springer, Berlin, pp. 345–364.

Govindaraju, K., 1994. Compilation of working values and sample description for 383 geostandards. Geostand. Newslet. 18, 1–158.

Graham, D.W., Bender, M.L., Williams, D.F., Keigwin, L.D.Jr., 1982. Strontium calcium ratios in Conocoic planktonic foraminifera. Geochim. Cosmochim. Acta 46, 1281–1292.

Hallam, A., 1992. Phanerozoic Sea-Level Changes. Columbia University Press, New York.

Hendriks, F., Luger, P., Strouhal, A., 1990. Early Tertiary marine palygorskite and sepiolite neoformation in SE Egypt. Z. Dtsch. Geol. Ges. 141, 87–97.

Herbert, T.D., Silva, I.P., Erba, E., Fischer, A.G., 1995. Orbital chronology of Cretaceous-Paleocene marine sediments. In: Berggren, W.A. et al. (Eds.), Time Scales and Global Stratigraphic Correlations. Soc. Econ. Paleontol. Mineral. Spec. Publ. 54, pp. 81–93.

Jenkyns, H.C., 1996. Relative sea-level change and carbon isotopes: data from the Upper Jurassic (Oxfordian) of central and Southern Europe. Terra Nova 8, 75–85.

Jenkyns, H.C., Gale, A.S., Corfield, R.M., 1994. Carbon- and oxygen-isotope stratigraphy of the English Chalk and Italian Scaglia and its palaeoclimatic significance. Geol. Mag. 131, 1–34.

Jenkyns, H.C., Mutterlose, J., Sliter, W.V., 1995. Upper Cretaceous carbon- and oxygen-isotope stratigraphy of deep-water sediments from the North-Central Pacific (Site 869, Flank of Pikinni-Wodejebato, Marshall Islands). Proc. ODP Sci. Results 143, 105–108.

Kaiho, K., Kajiwara, K., Tazaki, K., Ueshima, M., Takeda,

N., Kawahata, H., Arinobu, T., Ishiwatari, R., Hirai, A., Lamolda, M.A., 1999. Oceanic primary productivity and dissolved oxygen levels at the Creataceous-Tertiary boundary: Their decrease, subsequent warming and recovery. Paleoceanography 14, 511–524.

Karoui, N., Zaghbib-Turki, D., 1998. Une nouvelle coupe complète pur son passage Crétacé-Tertiaire: la coupe d'Elles, témoignage des foraminiféres planctoniques. In: International Workshop on Cretaceous-Tertiary Transition, Tunis, pp. 55–57.

Karoui-Yakoub, N., Keller, G., Zaghbib-Turky, D., 2002. The Cretaceous–Tertiary (K–T) mass extinction in planktic foraminifera at Elles I and El Melah. Tunisia. Palaeogeogr. Palaeoclimatol. Palaeoecol. 178, 233–255.

Karpoff, A.M., Lagabrielle, Y., Boillott, G., Girardeau, J., 1989. L'authigenèse océanique de palygorskite, par halmyrolyse de péridotites serpentinisées (marge de Galice): ses implications géodynamiques. C.R. Acad. Sci. Paris 308, 647–654.

Keller, G., 1988a. Biotic turnover in benthic foraminifera across the Cretaceous/Tertiary boundary at El Kef, Tunisia. Palaeogeogr. Palaeoclimatol. Palaeoecol. 66, 153–182.

Keller, G., 1988b. Extinction, survivorship and evolution of planktic foraminifera across the Cretaceous/Tertiary boundary at El Kef, Tunisia. Mar. Micropaleontol. 13, 239–263.

Keller, G., Adatte, T., Stinnesbeck, W., Luciani, V., Karoui-Yakoubi, N., Zaghbib-Turki, D., 2002. Paleoecology of the Cretaceous–Tertiary mass extinction in planktic foraminifera. Palaeogeogr. Palaeoclimatol. Palaeoecol. 178, 257–297.

Keller, G., Adatte, T., Stinnesbeck, W., Stüben, D., Kramar, U., Berner, Z., Li, L., von Salis Perch-Nielsen, K., 1998. The Cretaceous–Tertiary transition on the shallow Saharan Platform of Southern Tunisia. Geobios 30, 951–975.

Keller, G., Barrera, E., Schmitz, B., Mattson, E., 1993. Gradual mass extinction, species survivorship and long-term environmental changes across the Cretaceous/Tertiary boundary in high latitudes. Geol. Soc. Am. Bull. 105, 979–997.

Keller, G., Li, L., MacLeod, N., 1996. The Cretaceous Tertiary boundary stratotype at El Kef, Tunisia: How catastrophic was the mass extinction. Palaeogeogr. Palaeoclimatol. Palaeoecol. 119, 221–254.

Keller, G., Lindinger, M., 1989. Stable isotope, TOC, $CaCO_3$ record across the Creataceous/Tertiary boundary at El Kef, Tunisia. Palaeogeogr. Palaeoclimatol. Palaeoecol. 73, 243–265.

Keller, G., Stinnesbeck, W., 1996. Sea level changes, clastic deposits and megatsunamis across the Cretaceous–Tertiary boundary. In: MacLeod, N., Keller, G. (Eds.), Cretaceous–Tertiary Mass Extinctions. Norton Press, New York, pp. 415–450.

Knauer, G.A., Martin, J.H., 1982. Trace elements and primary production: Problems, effects and solutions. In: Wong, C.S., Boyle, E., Bruland, K.W., Burton, J.D., Goldberg, E.D. (Eds.), Trace Metals in Sea Water, NATO Conf. Ser. 9. Plenum Press, New York, pp. 825–840.

Kouwenhoven, T.J., Speijer, R.P., Van Oosterhout, C.W.M., Van Der Zwaan, G.J., 1997. Benthic foraminiferal assemblages between two major extinction events – the Paleocene El Kef section, Tunisia. Mar. Micropaleontol. 29, 105–127.

Kramar, U., 1984. First experiences with a tube-excited energy-dispersive X-ray fluorescence. J. Geochem. Explor. 21, 373–383.

Kramar, U., 1997. Advances in energy-dispersive X-ray fluorescence. J. Geochem. Explor. 58, 73–80.

Li, L., Keller, G., 1998. Maastrichtian climate, productivity and faunal turnovers in planktic foraminifera in South Atlantic DSDP Sites 525A and 21. Mar. Micropaleontol. 33, 55–86.

Li, L., Keller, G., Adatte, T., Stinnesbeck, W., 2000. Late Cretaceous sea level changes in Tunisia: A multi-disciplinary approach. J. Geol. Soc. London 157, 447–458.

Luciani, V., 2002. High resolution planktic foraminiferal analysis form the Cretaceous/Tertiary boundary at Ain Settara (Tunisia): Evidence of an extended mass extinction. Palaeogeogr. Palaeoclimatol. Palaeoecol. 178, 299–319.

MacLeod, N., Keller, G., 1991. Hiatus distribution and mass extinction at the Cretaceous/Tertiary boundary. Geology 19, 497–501.

McManus, J., Berelson, W.M., Klinkhammer, G.P., Johnson, K.S., Coale, K.H., Anderson, R.F., Kumar, N., Burdige, D.J., Hammond, D.E., Brummsack, H.J., McCorkle, D.C., Rushdi, A., 1998. Geochemistry of barium in marine sediments: Implications for its use as a paleoproxy. Geochim. Cosmochim. Acta 62, 3453–3473.

McManus, J., Berelson, W.M., Hammond, D.E., Klinkhammer, G.P., 1999. Barium cycling in the North Pacific: Implications for the utility of Ba as a paleoproductivity and paleoalkalinity proxy. Paleoceanography 14, 53–61.

Méon, H., 1990. Palynologic studies of the Cretaceous/Tertiary boundary interval at El Kef outcrop, north-western Tunisia: Paleogeographic implication. Rev. Paleobot. Palynol. 65, 85–94.

Mitchell, S.F., Ball, J.D., Crowley, S.F., Marshall, J.D., Paul, C.R.C., Veltkamp, C.J., Samir, A., 1997. Isotope data from cretaceous chalks and foraminifera: Environmental or diagenetic signals? Geology 25, 691–694.

Molina, E., Arenillas, I., Arz, J.A., 1998. Mass extinction in planktic foraminifera at the Cretaceous/Tertiary boundary in subtropical to temperate latitudes. Bull. Soc. Geol. France 169, 351–372.

Monaco, A., Mear, Y., Murat, A., Fernandez, J.M., 1982. Critères mineralogiques pour la reconnaissance des turbidites fines. C.R. Acad. Sci. Paris Ser. II 295, 43–46.

Murray, R.W., Leinen, M., 1996. Scavenged excess aluminum and its relationship to bulk titanium in biogenic sediment from central equatorial Pacific Ocean. Geochim. Cosmochim. Acta 60, 3869–3878.

Oberhänsli, H., Keller, G., Adatte, T., Pardo, A., 1998. Diagenetically and environmentally controled changes across a K/T transition at Koshak Mangyshlak (Kazakstan). Bull. Soc. Geol. France 169, 493–501.

Pardo, A., Ortiz, N., Keller, G., 1996. Latest Maastrichtian foraminiferal turnover and its environmental implications at Agost, Spain. In: MacLeod, N., Keller, G. (Eds.), Creta-

ceous-Tertiary Boundary Mass Extinction: Biotic and Environmental Changes. Norton Press, New York, pp. 139–172.
Pardo, A., Adatte, T., Keller, G., Oberhänsli, H., 1999. Paleoenvironmental changes across the Cretaceous-Tertiary boundary at Koshak, Kazakhstan, based on planktic foraminifera and clay mineralogy. Palaeogeogr. Palaeoclimatol. Palaeoecol. 154, 247–273.
Paul, C.R.C., Lamolda, M.A., Mitchell, S.F., Vaziri, M.R., Gorostidi, A., Marshall, J.D., 1999. The Cenomanian–Turonian boundary at Eastbourne (Sussex, U.K): a proposed European reference section. Palaeogeogr. Palaeoclimatol. Palaeoecol. 150, 83–121.
Perch-Nielsen, K., 1981. Les coccolithes du Paléocène près de El Kef, Tunisie, et leurs ancetres. Cah. Micropaléontol. 3, 7–23.
Perch-Nielsen, K, McKenzie, J.A., He, Q., 1982. Biostratigraphy and isotope stratigraphy and the 'catastropic' extinction of calcareous nannoplankton at the K/T boundary. In: Silver, L.T., Schulz, P.H. (Eds.), Geol. Soc. Am. Mem. 190, pp. 353–371.
Peypouquet, J.P., Grousset, F., Mourguiart, P., 1986. Paleoceanography of the Mesogean Sea based on ostracods of the northern Tunisian continental shelf between the late Cretaceous and early Paleogene. Geol. Rundsch. 75, 159–174.
Pospichal, J., 1994. Calcareous nannofossils at the K/T boundary, El Kef: No evidence of stepwise extinctions. Geology 22, 99–102.
Rathburn, A.E., Dedeckker, P., 1997. Magnesium and strontium compositions of recent benthic formainifera from the Coral Sea, Australia and Prydz Bay, Antarctica. Mar. Micropaleontol. 32, 231–248.
Remane, J., Keller, G., Hardenbol, J., Ben Haj Ali, M., 1999. International workshop on Cretaceous-Paleogene transitions in Tunisia: The El Kef stratotype for the Cretaceous-Paleogene boundary reconfirmed. Episodes 22, 47–48.
Robert, C., Chamley, H., 1991. Development of early Eocene warm climates, as inferred from clay mineral variations in oceanic sediments. Palaeogeogr. Palaeoclimatol. Palaeoecol. 89, 315–332.
Robert, C., Kennett, J.P., 1994. Antarctic subtropical humid episod at the Paleocene-Eocene boundary: Clay mineral evidence. Geology 22, 211–214.
Rocchia, R., Donze, P., Froget, L., Jehanno, C., Robin, E., 1995. L'iridium à la limite Crétacé-Tertiaire du site d'El Kef Tunisia. Ann. Mines Géol. 35, 103–120.
Rocchia, R., Robin, E., Pierrard, O., Lefevre, I., 2002. The stratigraphic distribution of iridium and Ni-rich spinels at the Cretaceous–Tertiary boundary of El Kef, Tunisia. Palaeogeogr. Palaeoclimatol. Palaeoecol. In press.
Rosenthal, Y., Boyle, E.D., Labeyrie, L., 1997a. Last glacial maximum paleochemistry and deepwater circulation in the Southern Ocean: Evidence from foraminiferal cadmium. Paleoceanography 12, 787–796.
Rosenthal, Y., Boyle, E.D., Slowley, N., 1997b. Temperature control on the incorporation of magnesium, strontium, fluorine and cadmium into benthic foraminiferal shells from Little Bahama Bank: Prospects for thermocline paleoceanography. Geochim. Cosmochim. Acta 61, 3633–3643.
Rühlemann, C., Frank, M., Hale, W., Mangini, A., Mulitza, S., Müller, P.J., Wefer, G., 1996. Late quarternary productivity changes in the western equatorial Atlantic: Evidence from ^{230}Th-normalised carbonate and organic carbon accumulation rates. Mar. Geol. 135, 127–152.
Saint-Marc, P., 1992. Biogeographic and bathymetric distribution of benthic foraminifera in Paleocene El Haria Formation of Tunisia. J. Afric. Earth Sci. 15, 473–487.
Schlanger, S.O., 1988. Strontium storage and release during deposition and diagenesis of marine carbonates related to sea level variations. In: Lerman, A., Meybeck, M. (Eds.), Physical and Chemical Weathering on Geochemical Cycles. Kluwer, Dordrecht, pp. 323–341.
Schmitz, B., Keller, G., Stenvall, O., 1992. Stable isotope and foraminiferal changes across the Cretaceous/Tertiary boundary at Stevns Klint, Denmark: Arguments for long-term oceanic instability before and after bolide impact. Palaeogeogr. Palaeoclimatol. Palaeoecol. 96, 233–260.
Schroeder, J.O., Murray, R.W., Leinen, M., Pflaum, R.C., Janecek, T.R., 1997. Barium in equatorial Pacific carboanate sediment: Terrigeous, oxide and biogenic associations. Paleoceanography 12, 125–146.
Shackelton, N.J., 1967. Oxygen isotope analyses and paleotemperatures reassessed. Nature 215, 15–17.
Shackelton, N.J., 1987. The carbon isotope record of the Cenozoic: History of organic carbon burial and of oxygen in the ocean and atmosphere. In: Brooks, J., Fleet, A.J. (Eds.), Marine Petroleum Source Rocks. Geol. Soc. London Spec. Publ. 26, pp. 423–434.
Shackelton, N.J., Imbire, J., Hall, M.A., 1983. Oygen and carbon isotope record of East Pacific core V19-30: implications for the formation of deep water in the late Pleistocene North Atlantic. Earth Planet. Sci. Lett. 65, 233–244.
Smit, J., 1982. Extinction and evolution of planktic foraminifera after a major impact at the Cretaceous/Tertiary boundary. Geol. Soc. Am. Spec. Pap. 190, pp. 329–352.
Spero, H.J., Bijma, J., Lea, D.W., Bemis, B.E., 1997. Effect of seawater carbonate concentration on foraminiferal carbon and oxygen isotopes. Nature 390, 497–499.
Stinnesbeck, W., Keller, G., Adatte, T., 1998. Lithological characteristics of the K/T transition in Tunisia: Evidence of a tsunami event? In: International Workshop on Cretaceous–Tertiary Transition, Tunis, pp. 53–55.
Stoll, H.M., Schrag, D.P., 1996. Evidence for glacial control of rapid sea level changes in the early cretaceous. Science 272, 1771–1774.
Stoll, H.M., Schrag, D.P., 1998. Effects of Quaternary sea level cycles on strontium in seawater. Geochim. Cosmochim. Acta 62, 1107–1118.
Stott, L.D., Kennet, J.P., 1990. The paleoceanographic and paleoclimatic signature of the Cretaceous/Paleogene boundary in the Antarctic: Stable isotope results from ODP Leg 113. In: Barker, P.F., Kennet, J.P. (Eds.). Proc. ODP Sci. Results 113, pp. 829–848.
von Breymann, M.T., Emeis, K.-C., Suess, E., 1992. Water depth and diagenetic constraints on the use of barium as palaeoproductivity indicator. In: Summerhayes, C.P., Prell,

W.L., Emeis, K.-C. (Eds.), Upwelling Systems: Evolution since Early Miocene. Geol. Soc. London Spec. Publ. 64, pp. 273–284.
Weaver, C.E., 1989. Clays, Muds and Shales. Development in Sedimentology 44. Elsevier, Amsterdam, 819 pp.
Zachos, J.C., Arthur, M.A., 1986. Paleoceanography of the Cretaceous/Tertiary boundary event: Inferences from stable isotopic and other data. Paleoceanography 1, 5–26.
Zachos, J.C., Arthur, M.A., Dean, W.A., 1989. Geochemical evidence for suppression of pelagic marine productivity at the Createceous/Tertiary boundary. Nature 337, 61–64.